Theoretical Notes
Note 206
February, 1975

Analytical Calculations on Photoelectron-Induced Currents on a Model of the FLTSATCOM Satellite

L. Marin, K. S. H. Lee and T. K. Liu

Dikewood Corporation, Westwood Research Branch
Los Angeles, California

Abstract

From a rigorous integral-equation formulation a simplified integro-differential equation is derived for the induced current on the boom of a FLTSATCOM satellite with the solar panels and the central cylinder replaced by some appropriate localized generators and lumped impedances driving and loading the boom. The induced currents result partly from (1) the motion of the photoelectrons near the satellite and partly from (2) the redistribution of the positive charges left behind by the ejected electrons. The simplified equation for the case of one moving electron is solved by the method of asymptotic expansion; explicit quasi-static as well as dynamic results are found both in time and frequency domain. It is found that the lowest resonance mode together with the quasi-static solution is sufficiently accurate for the photoelectron-induced currents on the FLTSATCOM satellite. The quasi-static solution for one electron is also utilized to obtain the low-fluence result for a given incident photon pulse, a given yield function (electrons per photon), and a given angular and energy distribution of the ejected electrons. Throughout the report, the results computed from explicit analytical solutions are graphically presented and physically interpreted.

PREFACE

Thanks go to Capt. R. L. Gardner and Lt. J. L. Gilbert for their many useful suggestions. The authors also wish to thank Dr. C. E. Baum for enlightening discussions.

CONTENTS

ILLUSTRATIONS

SECTION I

INTRODUCTION

The physical process in the creation of the system generated electromagnetic pulse (SGEMP) is rather involved. Among other things, it involves the geometry and composition of the system (e.g. a satellite). The importance of these two factors of the system can be understood if one can find a theoretical model which contains all the essential electromagnetic features of the system and yet is amenable to a reasonbly simple analytical treatment.

Many satellites can be modeled by simple nonresonant structures. A nonresonant structure is characterized by the large radiation damping possessed by the SGEMP induced currents and charges. One such simple nonresonant structure is a sphere, a detailed analysis of which has shown that a quasi-static (quasi-electrostatic and quasi-magnetostatic) approach is adequate for nonresonant structures for electron energies up to 2 MeV (reference 1). This result is quite valuable because the quasi-static approach has many computational advantages.

Other types of satellites are inherently resonant structures. A resonant structure is characterized by the continued oscillations of the SGEMP induced currents and charges without significant damping even long after the photon pulse has passed. One such resonant structure is a thin wire. By making the assumption that the wire radius is much smaller than the wire length, it is possible to obtain an explicit analytical solution of the SGEMP induced currents on the wire (see reference 2). An examination of the solution clearly shows that the resonance effect is significant even for moderately low electron energies, implying that the quasi-static approach to SGEMP calculations for a resonant structure is inadequate.

In this report, the thin-wire model will be extended so as to include other essential electromagnetic features of a FLTSATCOM satellite depicted in figure 1. Clearly, this satellite is a highly resonant structure with the capacitive solar panels and central cylinder resonating with the inductive boom. On physical grounds, one expects that these added capacitive features would introduce not only impedance loading but also localized current or

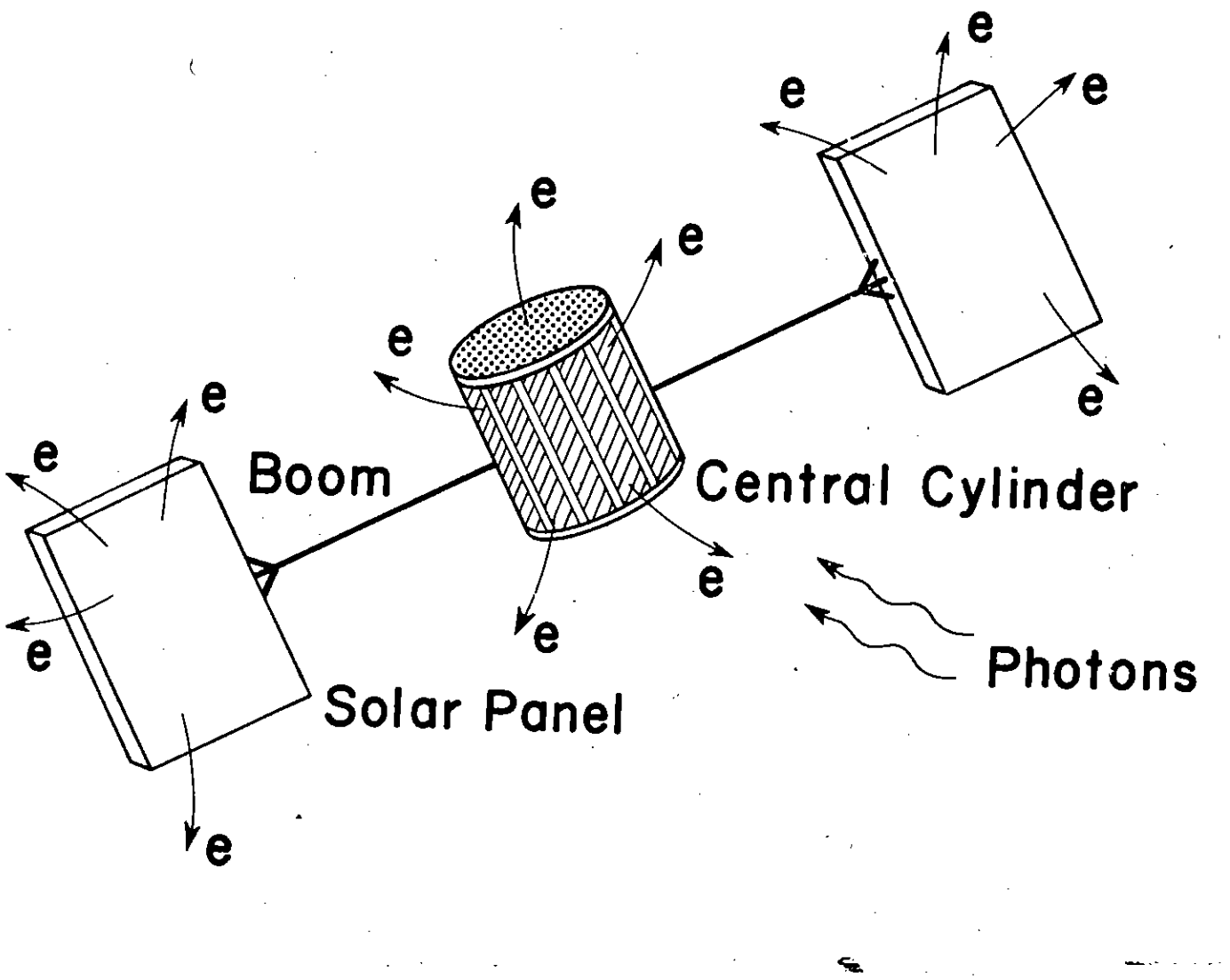

Figure 1. Photons Impinging on a FLTSATCOM Satellite

voltage generators into the thin-wire model studied in reference 2. The currents induced on the boom consist of two parts: one part is due to the motions of the electrons outside the satellite, and the other part is due to the redistribution of positive charges left behind by the ejected electrons on the solar panels and the central cylinder. In this report, these physical considerations will be put into a mathematical formulation from which analytical results can be deduced.

The usual procedure of solving SGEMP problems is followed in the present report. First, the one-electron problem is solved and the solution of this problem gives the so-called Green's function for the structure under consideration. Then, the currents and charges on the satellite induced by many moving electrons are obtained by using the calculated Green's function and the principle of superposition. Such a procedure is valid for low-fluence calculations where the mutual interactions among electrons are assumed to be negligible. Explicit results are obtained for a given incident photon pulse (triangular time dependence), a given yield function, and given energy and spatial distributions of the emitted photoelectrons.

A simplified integral equation for the induced currents on the satellite is derived in section II. This equation is then solved analytically for the one-electron problem, quasi-statically in section III and dynamically in section IV. It is observed from the calculated results that the satellite's response can be described accurately by the fundamental resonance mode alone for all electron energies of interest. This fundamental resonance can be found from a network representation of the satellite. The results obtained in sections III and IV are used in a low-fluence calculation in section V where the satellite's response to a given incident photon pulse is considered. In section VI, results are obtained of the induced currents resulting from the redistribution of the positive charges left behind on the satellite by the ejected photoelectrons. It is found that their contribution to the induced currents is comparable to that from the moving photoelectrons. Some other special aspects of the present SGEMP problem are considered in section VII. In the final section, section VIII, the results of this report are summarized and some natural extensions of the present study are given.

SECTION II

A SIMPLIFIED EQUATION FOR THE BOOM CURRENT

Although it is quite easy to write down an integral equation for the induced surface currents on the satellite shown in figure 1, this integral equation is so complicated that it is difficult to extract any useful information from it without spending an exorbitant amount of computer time on numerical computation. It is therefore of great value to have a simplified equation from which the induced currents can be calculated with relative ease and yet the results are physically interpretable and reasonably accurate.

The point of departure in deriving a simplified equation for the boom current is the well-known integro-differential equation for the surface current density $\underline{K}$ (reference 3)

$$\hat{n}\times\left(\frac{s^2}{c^2} - \nabla\nabla\cdot\right)\int_S \frac{\exp(-s|\underline{r}-\underline{r}'|/c)}{4\pi|\underline{r}-\underline{r}'|}\,\underline{K}(\underline{r}')dS' = s\varepsilon\hat{n}\times\underline{E}^{inc} \qquad (1)$$

where $\hat{n}$ is the outward unit normal of the surface S of the satellite. With the total current $I(z,s)$ along the boom in mind one can rewrite equation (1) as (see figure 2)

$$\left(\frac{d^2}{dz^2} - \frac{s^2}{c^2}\right)\int_0^{\ell} \frac{\exp(-sR/c)}{4\pi R}\, I(z',s)dz' = -s\varepsilon(E_z^{inc} + E_z^{sc}) \qquad (2)$$

where $R^2 = a^2 + (z-z')^2$, E_z^{inc} is the electric field tangential to the boom due to the ejected electrons and E_z^{sc} is the axial component of the electric field on the boom due to the induced charges and currents on the solar panels. In figure 2, the central cylinder shown in figure 1 has been deleted; its effect on the boom current will be discussed in section VII. "Exact" values of E_z^{sc} can be obtained by first evaluating the currents on the solar panels through a tedious numerical solution of equation (1) over the entire surface of the satellite. However, as will be shown later in this section, simple

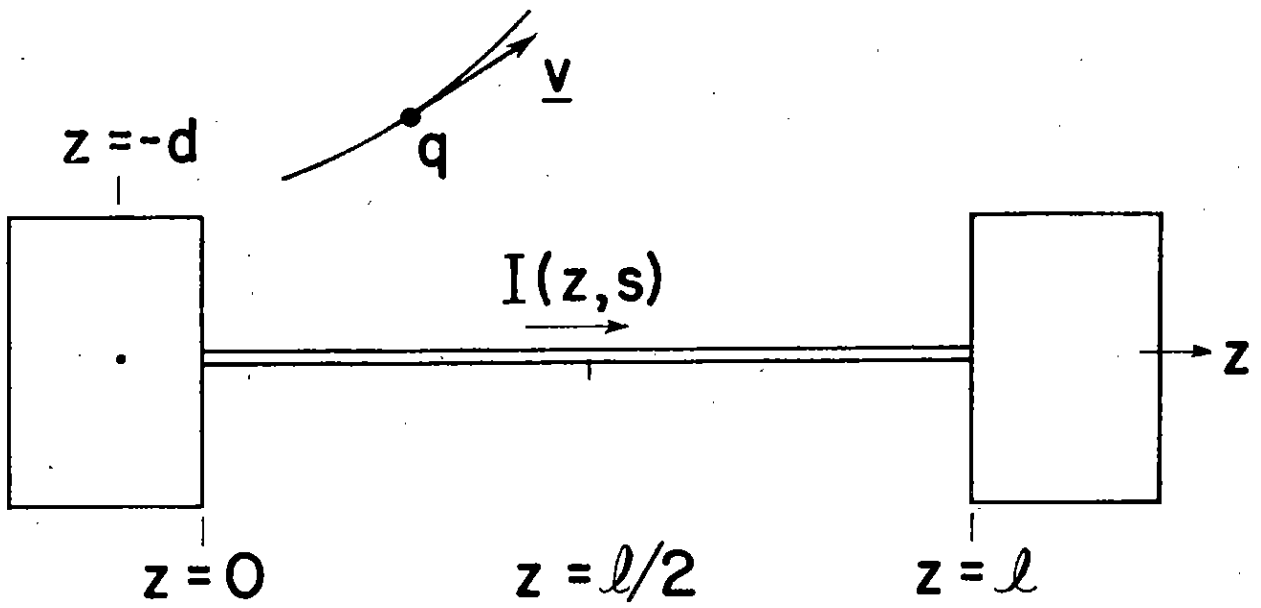

Figure 2. A Charge Moving Near a FLTSATCOM Satellite (with Central Cylinder Omitted)

approximate expressions for E_z^{sc} can be derived for use in equation (2). With this approximate E_z^{sc}, equation (2) is a simplified integro-differential equation for the boom current $I(z,s)$. It is perhaps appropriate here to mention that one can always write down an equation with the boom current as the only unknown by replacing the free-space Green's function in equation (2) by a much more complicated Green's function that satisfies the boundary conditions on the solar panels. The degree of difficulty in finding this Green's function is, however, the same as solving the entire scattering problem.

To solve equation (2) one needs to know the end conditions that $I(z,s)$ must satisfy at $z = 0,\ell$. A careful examination of an appropriate static problem valid near the intersection between the boom and the solar panels shows that the presence of the solar panels makes the linear charge density on the boom vanish at the intersection. Thus, from the continuity equation one then has the following end conditions:

$$\frac{dI}{dz} = 0 \qquad \text{at} \qquad z = 0,\ell \tag{3}$$

The scattered electric field E_z^{sc} can be viewed as the sum of two parts: (1) the electric field due to the net charge on each solar panel, and (2) the electric field due to the currents induced on each solar panel when it is isolated from the rest of the satellite structure. The solar panels of a typical FLTSATCOM satellite are electrically small for the dominating resonance frequencies of the structure, as will be justified from the results in later sections. Therefore, the current and charge distributions on them can be calculated by solving some appropriate quasi-static problems. Without going into great details, one can say from the solutions of such problems that the quasi-electrostatic field scattered from the solar panels is a localized field. Hence, it is reasonable to approximate E_z^{sc} in equation (2) by a strong electric field localized around the end points of the boom, viz.,

$$E_z^{sc} \simeq V_o'\delta(z) - V_\ell'\delta(z-\ell) + V_o''\delta(z) + V_\ell''\delta(z-\ell) \tag{4}$$

Here, V_o' (V_ℓ') is the potential on the solar panel at $z = 0$ ($z = \ell$) due to the net charge on the respective solar panel. In terms of the boom current one then has

$$V_o' = - I(0,s)/(sC_s), \qquad V_\ell' = I(\ell,s)/(sC_s) \tag{5}$$

and C_s is the capacitance of each solar panel. The quantity V_o'' (V_ℓ'') is proportional to the z-component of the incident electric field on the solar panel at $z = 0$ ($z = \ell$), viz.,

$$V_o'' = d E_z^{inc}(0,s), \qquad V_\ell'' = d E_z^{inc}(\ell,s) \tag{6}$$

A careful study of certain canonical problems shows that d is roughly the distance between the center point of the solar panel and the point at which the boom is connected to the solar panel.

Taking into account equations (4) and (5) one can write equation (2) in the following form:

$$\left(\frac{d^2}{dz^2} - \frac{s^2}{c^2}\right)\int_0^\ell \frac{\exp(-sR/c)}{4\pi R} I(z',s)dz' = \frac{\epsilon}{C_s}[I(0,s)\delta(z) + I(\ell,s)\delta(z-\ell)]$$

$$-s\epsilon[E_z^{inc}(z,s) + d E_z^{inc}(0,s)\delta(z)$$

$$+ d E_z^{inc}(\ell,s)\delta(z-\ell)] \tag{7}$$

which, together with the end conditions (3), forms a set of equations from which one can determine $I(z,s)$. The influence of the solar panels as manifested by the delta functions on the right-hand side of (7) can, alternatively, be incorporated in the end conditions. This can be accomplished by integrating each side of equation (7) over a small interval around the end points

$z = 0, \ell$ and expanding the left-hand side in the well-known asymptotic series. Thus, equation (7) and the boundary condition (3) for $I(z,s)$ can be replaced by the following integro-differential equation:

$$\left(\frac{d^2}{dz^2} - \frac{s^2}{c^2}\right)\int_0^{\ell} \frac{\exp(-sR/c)}{4\pi R} I(z',s)dz' = -s\varepsilon E_z^{inc}(z,s) \tag{8}$$

together with the new end conditions

$$\begin{aligned} \frac{d}{dz} I(0,s) &= \frac{C_b}{\ell C_s} I(0,s) - \frac{dC_b}{\ell} s E_z^{inc}(0,s) \\ \frac{d}{dz} I(\ell,s) &= -\frac{C_b}{\ell C_s} I(\ell,s) + \frac{dC_b}{\ell} s E_z^{inc}(\ell,s) \end{aligned} \tag{9}$$

where C_b is the capacitance of the boom, given by

$$C_b \simeq 4\pi\varepsilon \ell/\Omega, \qquad \Omega = 2 \ell n(\ell/a) \tag{10}$$

and a is the radius of the boom. The integro-differential equation (8) can be integrated to yield the following integral equation:

$$\int_0^{\ell} \frac{\exp(-sR/c)}{4\pi R} I(z',s)dz' = A \cosh\frac{sz}{c} + B \sinh\frac{sz}{c} - \frac{1}{2Z_o}\int_0^{\ell} \sinh(s|z-z'|/c)\, E_z^{inc}(z',s)dz' \tag{11}$$

and the unknown constants of integration A,B can be determined from the end conditions (9), and Z_o is the free-space wave impedance.

The following typical dimensions of the satellite will be used for the numerical calculations throughout this report: the boom length $\ell = 8\,\mathrm{m}$, the boom radius $a = 0.005\,\mathrm{m}$, the rectangular solar panel measures $2\,\mathrm{m} \times 3\,\mathrm{m}$, and the distance $d = 1\,\mathrm{m}$. Using these values, one obtains the following parameters: $\Omega = 14.8$, $C_b = 60.3\,\mathrm{pF}$ and $C_s = 97.8\,\mathrm{pF}$.

Equations (9) and (11) will be used in the following study of SGEMP induced currents on the boom. In section III these equations will be solved in the quasi-static limit, whereas in section IV they will be solved in the general case for a prescribed particle's path.

SECTION III

QUASI-STATIC SOLUTION

From a previous study of SGEMP induced currents on a thin wire (reference 2) it was observed that the quasi-static solution can be found by directly solving the reduced equation obtained from equation (8) by making c infinite. In the time domain the reduced equation becomes

$$\frac{\partial^2}{\partial z^2}\int_0^{\ell}\frac{I(z',t)}{4\pi R}\,dz' = -\epsilon\frac{\partial}{\partial t}E_z^{inc}(z,t) \tag{12}$$

together with the end conditions (9), which in the time domain are

$$\begin{aligned}\frac{\partial}{\partial z}I(0,t) &= \frac{C_b}{\ell C_s}I(0,t) - \frac{dC_b}{\ell}\frac{\partial}{\partial t}E_z^{inc}(0,t)\\ \frac{\partial}{\partial z}I(\ell,t) &= -\frac{C_b}{\ell C_s}I(\ell,t) + \frac{dC_b}{\ell}\frac{\partial}{\partial t}E_z^{inc}(\ell,t)\end{aligned} \tag{13}$$

Let the incident field be that of a moving particle with charge q and located at $\rho_o(t)$, $\phi_o(t)$, $z_o(t)$, outside the satellite. On the boom one then has

$$\begin{aligned}E_z^{inc}(z,t) &= \frac{q}{4\pi\epsilon}\frac{z-z_o}{R_o^3}, \qquad R_o^2 = \rho_o^2 + (z-z_o)^2\\ \frac{\partial}{\partial t}E_z^{inc}(z,t) &= \frac{-q}{4\pi\epsilon}\left[\frac{\dot z_o}{R_o^3} + \frac{3(z-z_o)^2\dot z_o}{R_o^5} - \frac{3(z-z_o)\rho_o\dot\rho_o}{R_o^5}\right]\end{aligned} \tag{14}$$

where the dot denotes time differentiation. Next, one inserts the expression

(14) into the right-hand side of the integro-differential equation (12) and uses the end conditions (13) to obtain the following asymptotic solution for the induced current at the center of the boom:

$$I(\ell/2,t) = -\frac{q}{2\Omega\ell}\left[\dot{z}_o\bar{I}_{||} + \dot{\rho}_o\bar{I}_{\perp} + \frac{C_s}{C_b}\left(\dot{z}_o\bar{I}'_{||} + \dot{\rho}_o\bar{I}'_{\perp}\right) + \frac{d}{\ell}\frac{C_s}{C_b}\left(\dot{z}_o\bar{I}''_{||} + \dot{\rho}_o\bar{I}''_{\perp}\right)\right] \tag{15}$$

where

$$\bar{I}_{||} = \frac{2}{[\eta^2 + (1/2-\xi)^2]^{1/2}} - \frac{1}{(\eta^2+\xi^2)^{1/2}} - \frac{1}{[\eta^2+(1-\xi)^2]^{1/2}}$$

$$\bar{I}'_{||} = \frac{\xi}{(\eta^2+\xi^2)^{3/2}} + \frac{1-\xi}{[\eta^2+(1-\xi)^2]^{3/2}}$$

$$\bar{I}''_{||} = \frac{\eta^2 - 2\xi^2}{(\eta^2+\xi^2)^{5/2}} + \frac{\eta^2 - 2(1-\xi)^2}{[\eta^2+(1-\xi)^2]^{5/2}}$$

(16)

$$\bar{I}_{\perp} = \frac{1}{\eta}\left[\frac{1-2\xi}{[\eta^2+(1/2-\xi)^2]^{1/2}} + \frac{\xi}{(\eta^2+\xi^2)^{1/2}} - \frac{1-\xi}{[\eta^2+(1-\xi)^2]^{1/2}}\right]$$

$$\bar{I}'_{\perp} = \frac{\eta}{(\eta^2+\xi^2)^{3/2}} - \frac{\eta}{[\eta^2+(1-\xi)^2]^{3/2}}$$

$$\bar{I}''_{\perp} = \frac{-3\xi\eta}{(\eta^2+\xi^2)^{5/2}} + \frac{3(1-\xi)\eta}{[\eta^2+(1-\xi)^2]^{5/2}}$$

and the dimensionless variables ξ and η are defined as

$$\xi = \frac{z_o}{\ell}, \qquad \eta = \frac{\rho_o}{\ell} \tag{17}$$

When the particle moves with velocity $\underline{v}$ that makes an angle θ with the positive z-axis so that

$$\underline{v} = \hat{z}\, v_{\parallel} + \hat{\rho}\, v_{\perp} = \hat{z} v \cos\theta + \hat{\rho} v \sin\theta \tag{18}$$

one can express the current $I(\ell/2,t)$ as

$$I(\ell/2,t) = -\frac{qv}{2\Omega\ell} [I_{\parallel} \cos\theta + I_{\perp} \sin\theta] \tag{19}$$

where

$$\begin{aligned} I_{\parallel} &= \bar{I}_{\parallel} + \frac{C_s}{C_b} \bar{I}'_{\parallel} + \frac{d}{\ell} \frac{C_s}{C_b} \bar{I}''_{\parallel} \\ I_{\perp} &= \bar{I}_{\perp} + \frac{C_s}{C_b} \bar{I}'_{\perp} + \frac{d}{\ell} \frac{C_s}{C_b} \bar{I}''_{\perp} \end{aligned} \tag{20}$$

For the satellite under study, $C_s/C_b \simeq 1.62$ and $d/\ell \simeq 0.125$. The normalized current components $I_{\parallel}$ and $I_{\perp}$ are plotted in figures 3 and 4. When the particle is moving parallel to the wire with constant speed v (so that $\theta = 0^o$) the coordinate ξ is proportional to the time t, since by choosing the time origin when the particle is right above one end $(z = 0)$ one has $\xi = vt/\ell$. On the other hand, when the particle is moving perpendicular to the wire with constant speed v (so that $\theta = 90^o$) the coordinate η is proportional to the time t such that $\eta = vt/\ell$.

1. ELECTRON LEAVING FROM A SOLAR PANEL

When the satellite is illuminated by a photon pulse, most photoelectrons are ejected from either the surfaces of the solar panels or from the surface

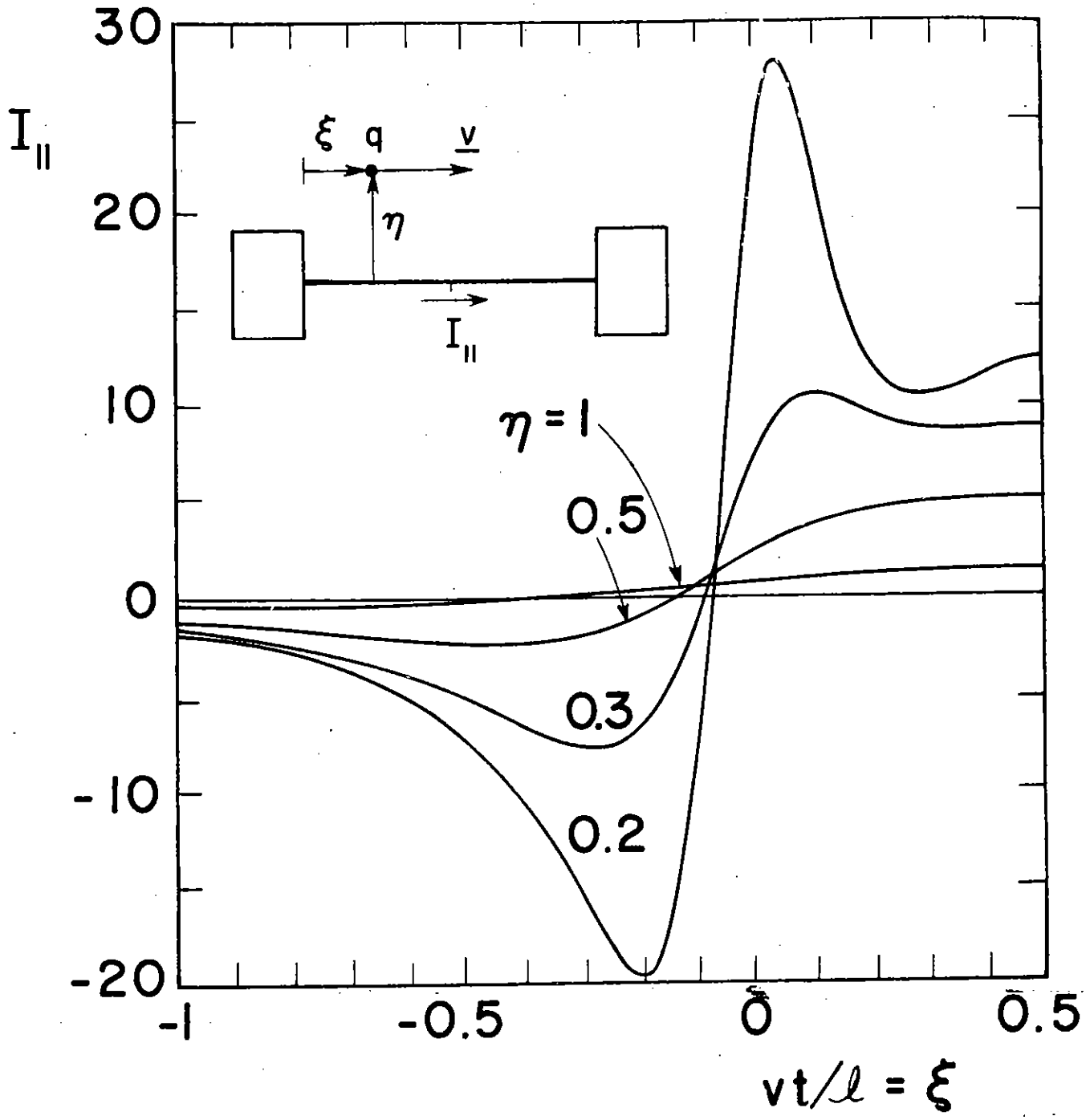

Figure 3. Normalized Current for Parallel Motion

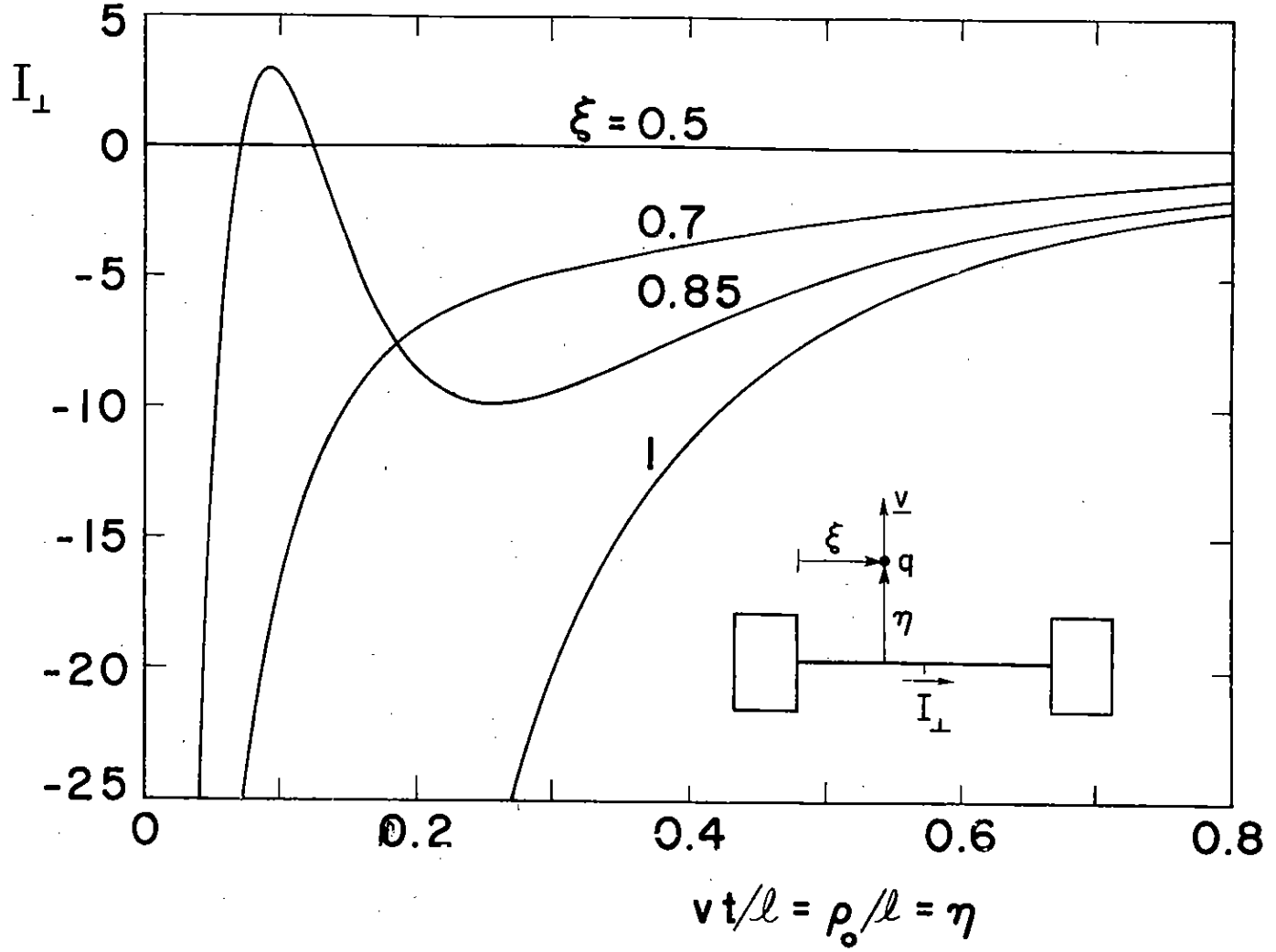

Figure 4. Normalized Current for Perpendicular Motion

of the central cylinder. The path of an electron leaving the solar panel at $z = 0$ with constant velocity $\underline{v}$ that makes an angle θ with respect to the positive z-axis can be described by

$$z = vt \cos\theta, \quad \rho = vt \sin\theta, \quad 0 \leq \theta \leq \pi$$

or (21)

$$\xi = \tau \cos\theta, \quad \eta = \tau \sin\theta, \quad \tau = vt/\ell$$

The current at the center of the boom induced by this electron is obtained by substituting the expressions (21) for ξ and η into equations (19) and (20). The time history of this current is shown in figure 5 where the normalized current I_s,

$$I_s(\tau) = I_{\parallel} \cos\theta + I_{\perp} \sin\theta \tag{22}$$

is plotted versus τ. From this figure one notes that the induced current is relatively insensitive to the angle θ at which the photoelectron is emitted. This is particularly true for the case where $\theta > 90^{\circ}$, i.e., the electron moves away from the satellite. Physically, this insensitivity to θ can be expected since the main interaction between the satellite and the electron takes place at the solar panel from which the electron is emitted.

2. ELECTRON LEAVING FROM THE CENTER OF THE BOOM

The path of an electron that leaves the center of the boom at $t = 0$ and moves with constant speed v at an angle θ with respect to the positive z-axis is

$$z = \ell/2 + vt \cos\theta, \quad \rho = vt \sin\theta, \quad 0 \leq \theta \leq \pi$$

or (23)

$$\xi = 1/2 + \tau \cos\theta, \quad \eta = \tau \sin\theta, \quad \tau = vt/\ell$$

The current induced at the center of the boom is again obtained from equation (19). The normalized current I_c,

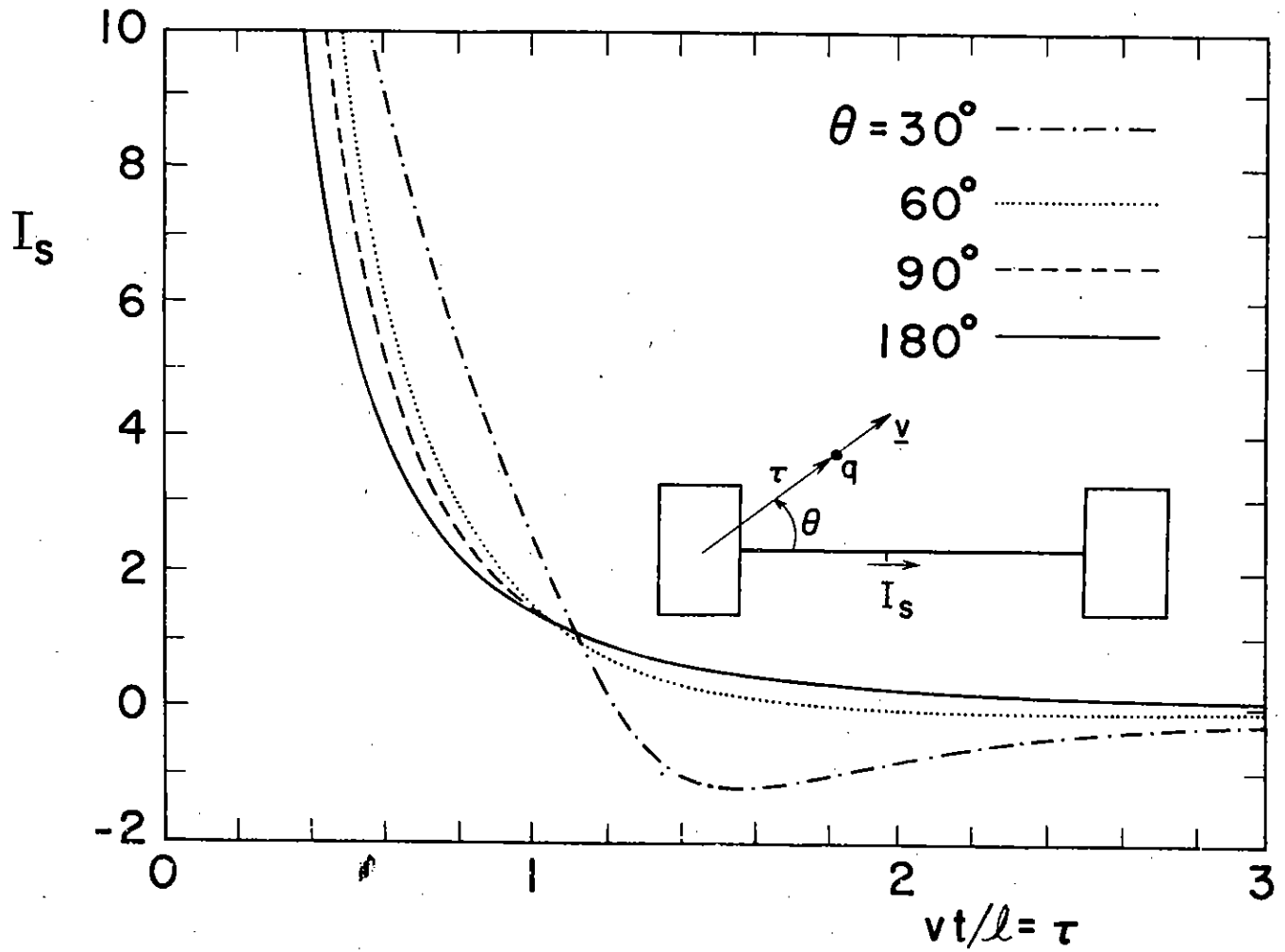

Figure 5. Normalized Current Induced by a Charge Ejected from one Solar Panel

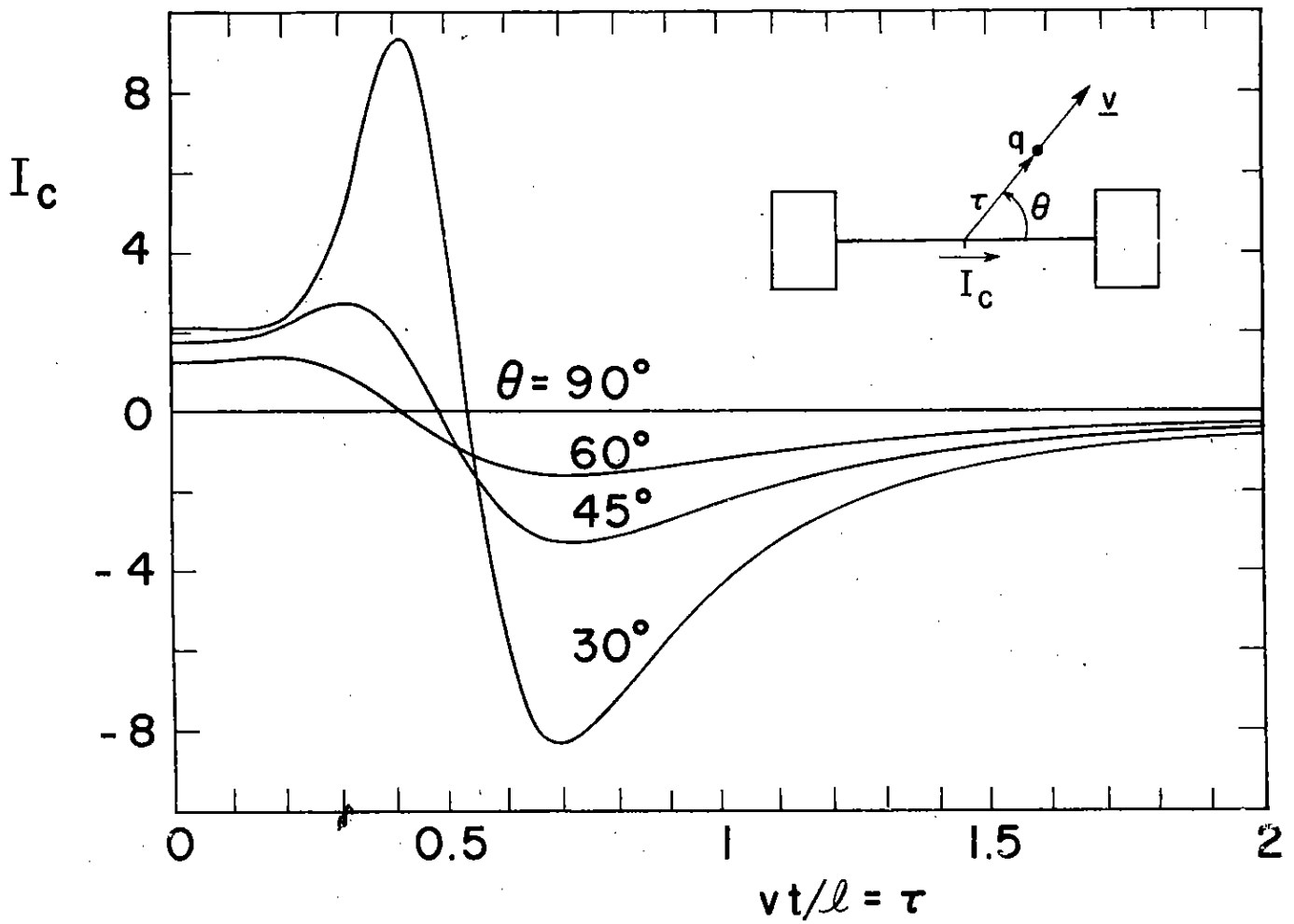

Figure 6. Normalized Current Induced by a Charge Ejected from the Central Cylinder

$$I_c(\tau) = I_{\parallel} \cos\theta + I_{\perp} \sin\theta \qquad (24)$$

is graphed in figure 6 versus τ for different values of θ. The symmetry of the problem implies that only the case $\theta \leq 90^{\circ}$ is needed.

3. FREQUENCY SPECTRUM OF PARALLEL MOTION

The quasi-static calculations have so far been restricted to the time-domain response of the current. In the quasi-static approximation the induced current depends only on the instantaneous position and velocity of the particle. To get the frequency-domain response, however, one has to specify the entire path when taking the two-sided Laplace (Fourier) transform of the time-domain response. When the particle moves with constant velocity parallel to the boom one gets the following frequency-domain response:

$$I(\ell/2,s) = \int_{-\infty}^{\infty} I(\ell/2,t)e^{-st}dt$$

$$= \frac{2q}{\Omega} K_o(\pm i\rho_o s/v)e^{-s\ell/2v} \left\{ \cosh(s\ell/2v) - 1 + [(s\ell/v)\sinh(s\ell/2v) \right.$$

$$\left. + (d\ell s^2/v^2)\cosh(s\ell/2v)]C_s/C_b \right\} \qquad (25)$$

where $K_o(x)$ is the modified Bessel function of the second kind and the $+(-)$ sign is used for $\mathrm{Im}\{s\}$ positive (negative). Observe that $I(\ell/2,s)$ is actually a function of $s\ell/v$. The variation of the induced current with $\omega(= is)$ is shown in figure 7 where the absolute value of the normalized quantity

$$I_{\omega} = (\Omega/2q)I(\ell/2,-i\omega)$$

$$= K_o(\pm \rho_o\omega/v)\, e^{i\omega\ell/2v} \left\{ \cos(\omega\ell/2v) - 1 - [(\omega\ell/v)\sin(\omega\ell/2v) \right.$$

$$\left. - (d\ell\omega^2/v^2)\cos(\omega\ell/2v)]C_s/C_b \right\} \qquad (26)$$

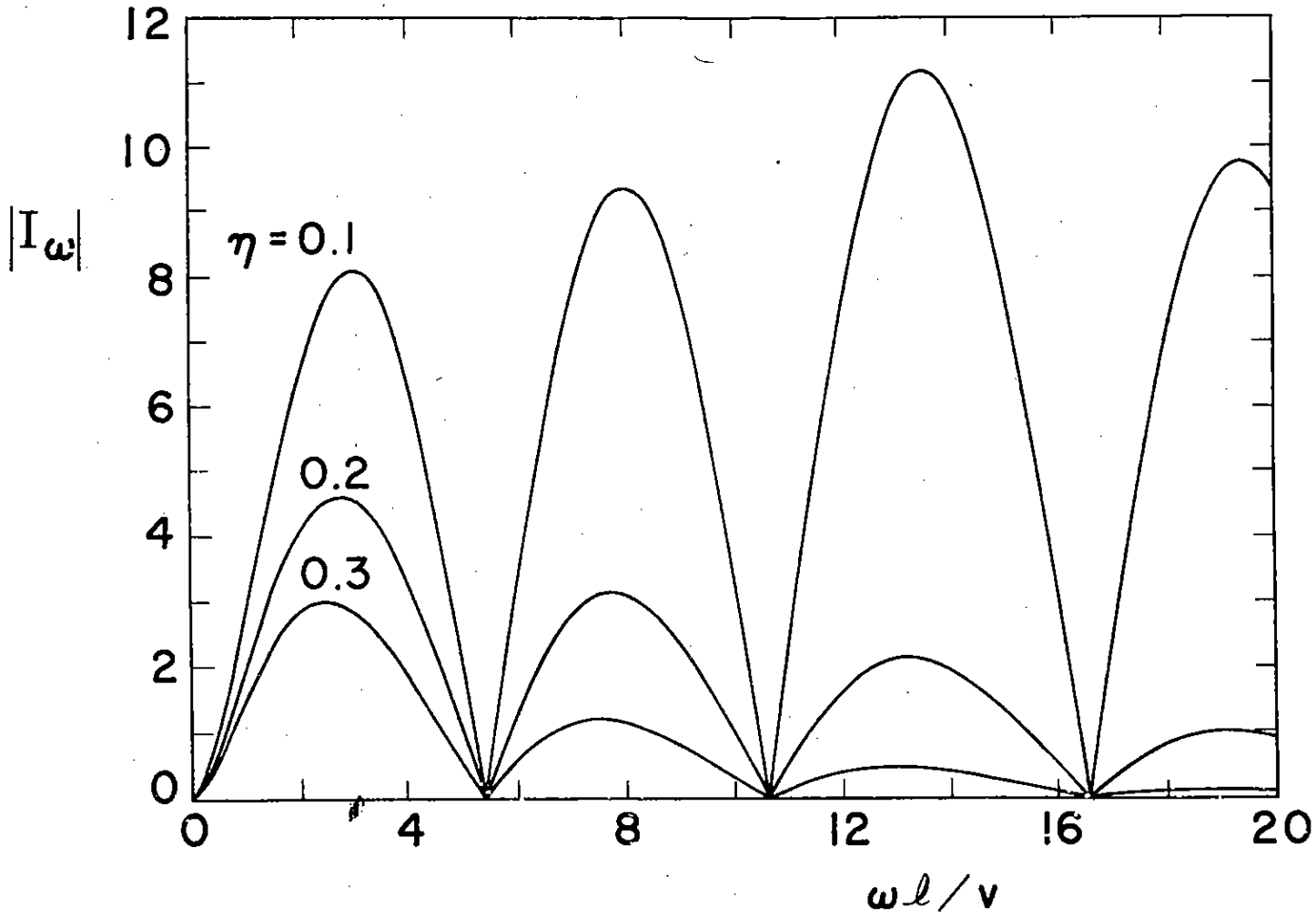

Figure 7. Frequency Variation of the Normalized Current for Parallel Motion

is plotted for $0 < \omega\ell/v < 20$. The nonresonant character of the quasi-static solution is clearly seen from figure 7.

SECTION IV

DYNAMIC SOLUTION

In the quasi-static solution it is assumed that all phenomena vary slowly in time and all oscillations are neglected. It is intuitively clear that this assumption is valid for very slowly moving electrons. In order to establish the quantitative accuracy of the quasi-static solution the full-fledged dynamic Maxwell equations for one particular choice of the electron's path will be solved in this section.

The boom current in the s-domain is obtained by solving either the integro-differential equation (7) or the integral equation (11) together with the end conditions (9). Using the general theory of scattering from finite-size bodies (the natural-mode method) one can cast the solution of equation (7) into the following form (reference 4):

$$I(z,s) = -\varepsilon s \sum_n \frac{1}{s-s_n} \frac{C_n}{B_n} I_n(z) \tag{27}$$

Here, s_n are the natural frequencies and they are those values of s at which equations (9) and (11) (and, of course, also equation (7)) have a non-trivial homogeneous solution, i.e., a nontrivial solution when $E_z^{inc} \equiv 0$. The corresponding homogeneous solution is denoted by $I_n(z)$, which is the current distribution of the natural mode with the resonance frequency s_n. Furthermore, in equation (27), (c.f. reference 5) one has

$$C_n = \int_0^{\ell} E_z^{inc}(z,s) I_n(z) dz + dE_z^{inc}(0,s) I_n(0) + dE_z^{inc}(\ell,s) I_n(\ell)$$

$$B_n \simeq -\frac{s_n \Omega}{2\pi c^2} \int_0^{\ell} I_n^2(z) dz \tag{28}$$

1. NATURAL MODES

To find the natural modes one solves the following eigenvalue problem: Find the values s_n of s, at which the following equations have a nontrivial solution:

$$\int_0^{\ell} \frac{\exp(-sR/c)}{4\pi R} I(z',s)dz' = A \cosh \frac{sz}{c} + B \sinh \frac{sz}{c}$$

$$\frac{d}{dz} I(0,s) = \frac{C_b}{\ell C_s} I(0,s), \quad \frac{d}{dz} I(\ell,s) = -\frac{C_b}{\ell C_s} I(\ell,s) \tag{29}$$

From the symmetry of the problem it is clear that the solution $I_n(z) \equiv I(z,s_n)$ is either an even or odd function of z about the point $z = \ell/2$ (the center point of the boom). An application of the asymptotic theory for solving thin-wire scattering problems to equation (29) gives the following first-order solution (c.f. reference 6):

$$I_n^e(z) = \cosh[s_n^e(z-\ell/2)/c], \quad \text{even modes}$$

$$I_n^o(z) = \sinh[s_n^o(z-\ell/2)/c], \quad \text{odd modes} \tag{30}$$

where the unimportant unknown multiplicative constants have been left out. The end conditions require that the natural frequencies be given by the roots of the transcendental equations

$$s_n^e: \quad \frac{s\ell}{c} \tanh \frac{s\ell}{2c} + \frac{C_b}{C_s} = 0, \quad \text{even modes}$$

$$s_n^o: \quad \frac{s\ell}{c} \coth \frac{s\ell}{2c} + \frac{C_b}{C_s} = 0, \quad \text{odd modes} \tag{31}$$

For large values of $|s|$ one can expand s_n^e and s_n^o in the following asymptotic series:

$$s_{n+1}^{e} \simeq \pm \frac{ic}{\ell}\left[2n\pi + 2\frac{C_b}{C_s}\frac{1}{2n\pi} - 4\left(\frac{C_b}{C_s}\right)^3\left(\frac{C_s}{C_b}+\frac{1}{6}\right)\frac{1}{(2n\pi)^3}\right]$$

$$s_{n}^{o} \simeq \pm \frac{ic}{\ell}\left[(2n-1)\pi + 2\frac{C_b}{C_s}\frac{1}{(2n-1)\pi} - 4\left(\frac{C_b}{C_s}\right)^3\left(\frac{C_s}{C_b}+\frac{1}{6}\right)\frac{1}{[(2n-1)\pi]^3}\right] \tag{32}$$

Using the capacitance values given in section II, one obtains the following values of the ten lowest resonances:

$$s_n^e = \pm i\omega_n^e = \pm i(c/\ell)\nu_n^e, \qquad s_n^o = \pm i\omega_n^o = \pm i(c/\ell)\nu_n^o \tag{33}$$

n	1	2	3	4	5	6	7	8	9	10
ν_n^e	1.06	6.47	12.66	18.91	25.18	31.46	37.73	44.01	50.29	56.57
ν_n^o	3.49	9.55	15.79	22.05	28.32	34.59	40.87	47.15	53.43	59.71

It should be pointed out that the asymptotic forms (32) agree within 0.5% with the numerical solution of equation (31) for all the roots except the lowest ones (n = 1).

Comparing the normalized resonance frequencies of the satellite to those of a straight wire, which are, in the first approximation, given by

$$\nu_n^e\Big|_{\text{wire}} = (2n-1)\pi, \qquad \nu_n^o\Big|_{\text{wire}} = 2n\pi, \qquad n \neq 0$$

one observes that numerically, the resonance frequencies of the satellite are

smaller than the corresponding ones of the straight wire. Thus, the solar panels have the effect of decreasing the resonance frequencies, as expected. This effect is most pronounced for the fundamental resonance whose resonance frequency ν_1^e is lowered by a factor of three with the add-on of the solar panels. The corresponding current distribution I_1^e of the lowest mode is given by

$$I_1^e(z) = \cos\left(0.53\,\frac{2z-\ell}{\ell}\right) \tag{34}$$

From equation (34) it can be seen that I_1^e takes its maximum value at $z = \ell/2$ and drops only 14% at the end points $z = 0,\ell$. Since I_1^e hardly varies along the boom one may use concepts in circuit theory to determine the resonance frequency of this mode. However, it should be emphasized that only the lowest resonance can be obtained from circuit analysis. All other modes are determined from the solution of a boundary-value problem. The lowest resonance can be determined approximately from an LC network where L is the inductance of the boom and C is the capacitance between the solar panels. With the dimensions and parameters given in section II one has

$$L \simeq \mu\ell\Omega/4\pi \simeq 1.18\times10^{-5} \quad \text{henry}$$

$$C \simeq \frac{1}{2\left[\frac{1}{C_s} - \frac{1}{4\pi\epsilon\ell}\right]} \simeq 5.50\times10^{-11} \quad \text{farad}$$

from which the normalized resonance frequency ν_1^e is found to be

$$\nu_1^e \simeq 1.05 \tag{35}$$

which agrees with the previous result to within 1%.

In the lowest-order solution of equations (29) the damping of each natural mode is neglected. To incorporate the damping into the expression for the resonance frequencies one has to continue to the next higher order

approximation to the solution of equations (29), or alternatively, one can use the concept of equivalent length and then invoke the damping formula of a straight wire (reference 7). By using the latter method the following first-order approximation of the damping constants α_n of the natural modes is obtained:

$$\alpha_n^e \equiv \frac{c}{\ell}\,\delta_n^e = \frac{\nu_n^e c}{(2n-1)\pi\Omega\ell}\left[\ell n[(2n-1)2\pi\Gamma] - Ci[(2n-1)2\pi]\right]$$

$$\alpha_n^o \equiv \frac{c}{\ell}\,\delta_n^o = \frac{\nu_n^o c}{2n\pi\Omega\ell}\left[\ell n(4n\pi\Gamma) - Ci(4n\pi)\right] \tag{36}$$

where $Ci(x)$ is the cosine integral and $\Gamma = 1.781...$ is the exponential of Euler's constant.

2. FREQUENCY VARIATION OF THE BOOM CURRENT

The resonances are uniquely determined by the satellite structure, but the excitation of each resonant mode depends also on the incident field, as shown in equation (28).

Here and henceforth, the incident electric field $E_z^{inc}(z,t)$ on the boom is specified to be that of a charge moving with constant speed parallel to the boom. Thus, one has

$$E_z^{inc}(z,t) = -\frac{q}{4\pi\varepsilon}\,\frac{\gamma(vt-z)}{[\rho_o^2 + \gamma^2(vt-z)^2]^{3/2}} \tag{37}$$

where $\gamma = (1-\beta^2)^{-1/2}$, $\beta = v/c$ and ρ_o is the transverse distance of the charge from the boom axis (see figure 2). The time origin is so defined that the particle is right above one end $(z = 0)$ of the wire at $t = 0$. The two-sided Laplace transform of equation (37) gives

$$E_z^{inc}(z,s) = \begin{cases} \frac{q}{2\pi\varepsilon} \frac{e^{-sz/v}}{\gamma v \rho_o} \frac{\rho_o s}{\gamma v} K_o[i\rho_o s/(\gamma v)], & \mathrm{Im}\{s\} > 0 \\ \frac{q}{2\pi\varepsilon} \frac{e^{-sz/v}}{\gamma v \rho_o} \frac{\rho_o s}{\gamma v} K_o[-i\rho_o s/(\gamma v)], & \mathrm{Im}\{s\} < 0 \end{cases} \tag{38}$$

Substituting the expressions (30) and (38) into equation (28) and evaluating the resulting integrals one obtains the following expressions for $\mathrm{Im}\{s\} < 0$:

$$C_n^e = \int_0^\ell E_z^{inc}(z,s) I_n^e(z)dz + d\,E_z^{inc}(0,s) I_n^e(0) + d\,E_z^{inc}(\ell,s) I_n^e(\ell)$$

$$= \frac{q}{2\pi\varepsilon} \frac{s}{\gamma^2 v^2} K_o[i\rho_o s/(\gamma v)] \left\{ \left[\frac{\sinh[(s_n^e \ell/2c) - (s\ell/2v)]}{(s_n^e/c) - (s/v)} \right. \right.$$

$$\left. \left. + \frac{\sinh[(s_n^e \ell/2c) + (s\ell/2v)]}{(s_n^e/c) + (s/v)} \right] e^{-s\ell/2v} + d\left[e^{-s\ell/v} + 1 \right] \cosh(s_n^e \ell/2c) \right\} \tag{39}$$

$$C_n^o = \int_0^\ell E_z^{inc}(z,s) I_n^o(z)dz + d\,E_z^{inc}(0,s) I_n^o(0) + d\,E_z^{inc}(\ell,s) I_n^o(\ell)$$

$$= \frac{q}{2\pi\varepsilon} \frac{s}{\gamma^2 v^2} K_o[i\rho_o s/(\gamma v)] \left\{ \left[\frac{\sinh[(s_n^o \ell/2c) - (s\ell/2v)]}{(s_n^o/c) - (s/v)} \right. \right.$$

$$\left. \left. - \frac{\sinh[(s_n^o \ell/2c) + (s\ell/2v)]}{(s_n^o/c) + (s/v)} \right] e^{-s\ell/2v} + d\left[e^{-s\ell/v} - 1 \right] \sinh(s_n^o \ell/2c) \right\}$$

For $\mathrm{Im}\{s\} > 0$ one simply replaces $K_o[i\rho_o s/(\gamma v)]$ by $K_o[-i\rho_o s/(\gamma v)]$ in equation (39). It now remains to determine B_n before equation (27) can be used to evaluate the frequency variation of the induced boom current. The integrals in equation (28) can be easily evaluated with the expressions (30) for the induced current. Thus,

$$B_n^e = -\frac{\Omega \ell s_n^e}{4\pi c^2}\left[1 + \frac{\sinh(s_n^e \ell/c)}{s_n^e \ell/c}\right]$$

$$B_n^o = -\frac{\Omega \ell s_n^o}{4\pi c^2}\left[1 - \frac{\sinh(s_n^o \ell/c)}{s_n^o \ell/c}\right] \tag{40}$$

The induced boom current is then given by

$$I(z,s) = \frac{2q}{\beta^2\gamma^2\Omega} K_o[i\rho_o s/(\gamma v)]e^{-s\ell/(2v)}$$

$$\left\{\sum_n \frac{s^2}{s_n^e(s-s_n^e)}\left[\frac{\sinh[(s_n^e - s/\beta)\ell/2c]}{(s_n^e - s/\beta)\ell/c} + \frac{\sinh[(s_n^e + s/\beta)\ell/2c]}{(s_n^e + s/\beta)\ell/c}\right.\right.$$

$$\left. + \frac{2d}{\ell}\cosh(s\ell/2\beta c)\cosh(s_n^e\ell/2c)\right]\frac{\cosh[s_n^e(2z-\ell)/2c]}{1 + (c/\ell s_n^e)\sinh(s_n^e\ell/c)}$$

$$+\sum_n \frac{s^2}{s_n^o(s-s_n^o)}\left[\frac{\sinh[(s_n^o - s/\beta)\ell/2c]}{(s_n^o - s/\beta)\ell/c} - \frac{\sinh[(s_n^o + s/\beta)\ell/2c]}{(s_n^o + s/\beta)\ell/c}\right.$$

$$\left.\left. - \frac{2d}{\ell}\sinh(s\ell/2\beta c)\sinh(s_n^o\ell/2c)\right]\frac{\sinh[s_n^o(2z-\ell)/2c]}{1 - (c/\ell s_n^o)\sinh(s_n^o\ell/c)}\right\}$$

$$\mathrm{Im}\{s\} < 0 \tag{41}$$

On physical grounds, it is expected that the current is large near the center of the boom and so it is of special importance to know the current at $z = \ell/2$. Since the current distribution of the odd modes vanishes at the center point one gets the following expression for the induced current at $z = \ell/2 (s = -i\omega)$:

$$I(\ell/2,\omega) = \frac{4q}{\beta^2\gamma^2\Omega} K_o[\rho_o\omega/(\gamma v)]e^{i\omega\ell/(2v)}$$

$$\sum_{n=1}^{\infty} \frac{\omega^2}{(\omega+i\alpha_n^e)^2 - (\omega_n^e)^2} \left[\frac{\sin[(\omega\ell/v - \nu_n^e)/2]}{\omega\ell/v - \nu_n^e} + \frac{\sin[(\omega\ell/v + \nu_n^e)/2]}{\omega\ell/v + \nu_n^e} \right.$$

$$\left. + \frac{2d}{\ell} \cos(\omega\ell/2v)\cos(\nu_n^e/2) \right] \frac{\nu_n^e}{\nu_n^e + \sin \nu_n^e} \qquad (42)$$

When ω is real and near the resonance frequency ω_n^e, the most important term in the sum (42) is

$$I(\ell/2,\omega) \approx \frac{2q}{\beta^2\gamma^2\Omega} K_o[\rho_o\omega_n^e/(\gamma v)]e^{i\omega_n^e\ell/(2v)}$$

$$\frac{\omega_n^e}{\omega - \omega_n^e + i\alpha_n^e} \left[\frac{\sin[\nu_n^e(1-\beta)/2\beta]}{\nu_n^e(1-\beta)/\beta} + \frac{\sin[\nu_n^e(1+\beta)/2\beta]}{\nu_n^e(1+\beta)/\beta} \right.$$

$$\left. + \frac{2d}{\ell} \cos(\nu_n^e/2\beta)\cos(\nu_n^e/2) \right] \frac{\nu_n^e}{\nu_n^e + \sin \nu_n^e} \qquad (43)$$

where, as before, $\nu_n^e = \ell\omega_n^e/c$.

On the other hand, when $|\omega - \omega_n^e| >> \alpha_n^e$ the "damping contribution" to s_n^e can be neglected and s_n^e can be approximated by $s_n^e \simeq \pm i\omega_n^e$. The simplified sum thus obtained can be summed in a closed form to yield the following expression:

$$I(\ell/2,\omega) = \frac{2q}{\ell} K_o[\rho_o\omega/(\gamma v)]e^{i\omega\ell/(2v)}$$

$$\left\{\sin(\omega\ell/2v) - \beta \sin(\omega\ell/2c) - [vC_b/(\omega\ell C_s)][\cos(\omega\ell/2v) - \cos(\omega\ell/2c)]\right.$$

$$\left. + (d\omega/c\gamma^2)\cos(\omega\ell/2v)\right\} \left\{\beta\left[\sin(\omega\ell/2c) - [cC_b/(\omega\ell/C_s)]\cos(\omega\ell/2c)\right]\right\}^{-1} \tag{44}$$

As expected, the denominator in equation (44) vanishes at $\omega = \omega_n^e$.

The frequency variation of the current at the midpoint of the boom is graphed in figures 8a - 8c. In these figures the normalized quantity

$$\mathfrak{I}(\omega) = \frac{\Omega}{2q} |I(\ell/2,\omega)| \tag{45}$$

is presented. From these figures one notes that the induced current has a very strong peak around the lowest resonance. In fact, the graphes show that for electron velocities less than $c/3$ only the lowest resonance is important. For higher velocities the second resonance gets somewhat more important but still its magnitude is 5 times less than the magnitude of the fundamental resonance for $\beta = 0.5$. These results show that for most SGEMP calculations involving this type of satellite one can limit his attention only to the lowest resonance.

3. TIME HISTORY OF THE BOOM CURRENT

The time variation of the induced current is obtained by taking an inverse Laplace transform of the expression (41). Following the same procedure as the one used in reference 2 one gets the following expression:

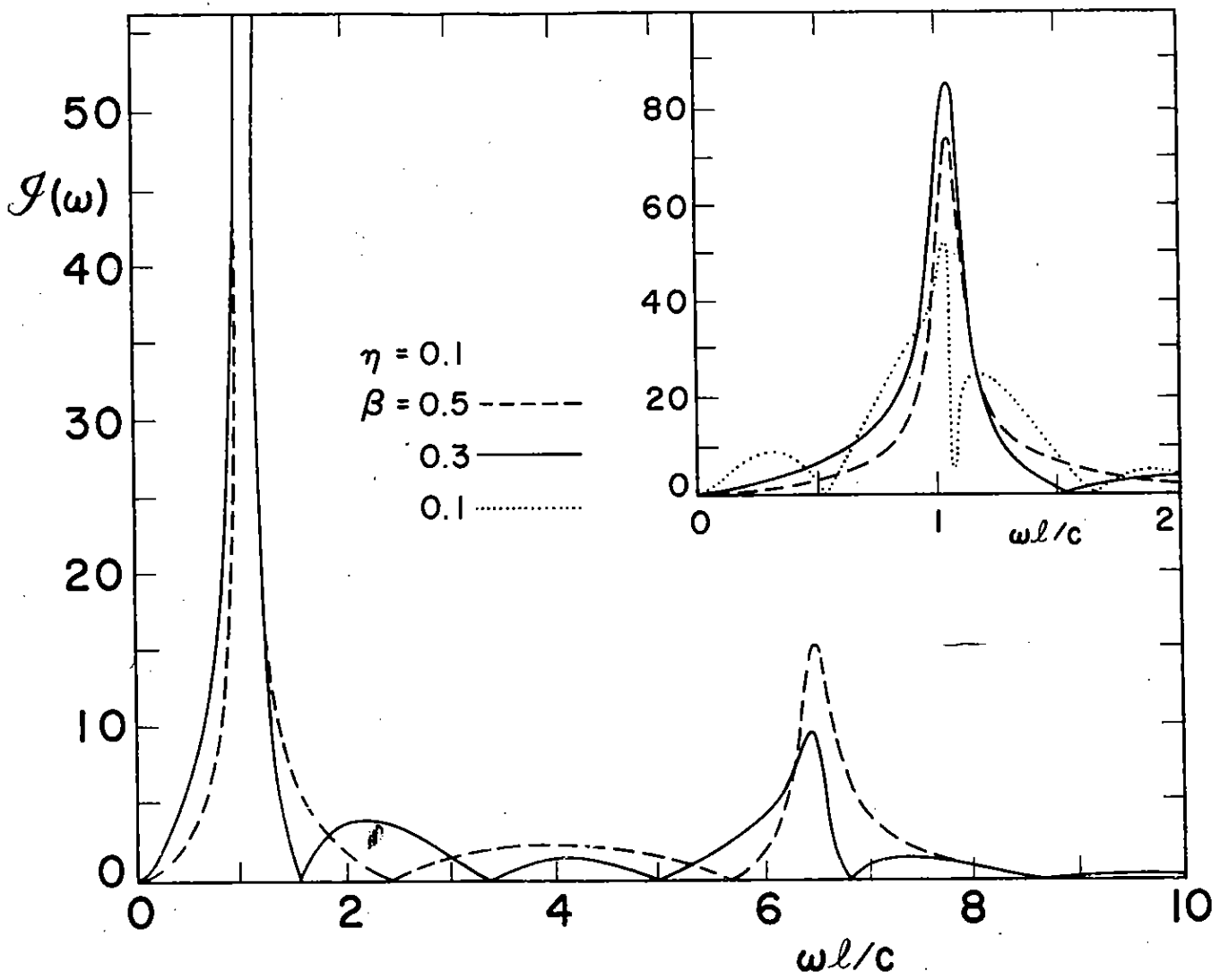

Figure 8a. Frequency Variation of Induced Current for $\eta = 0.1$

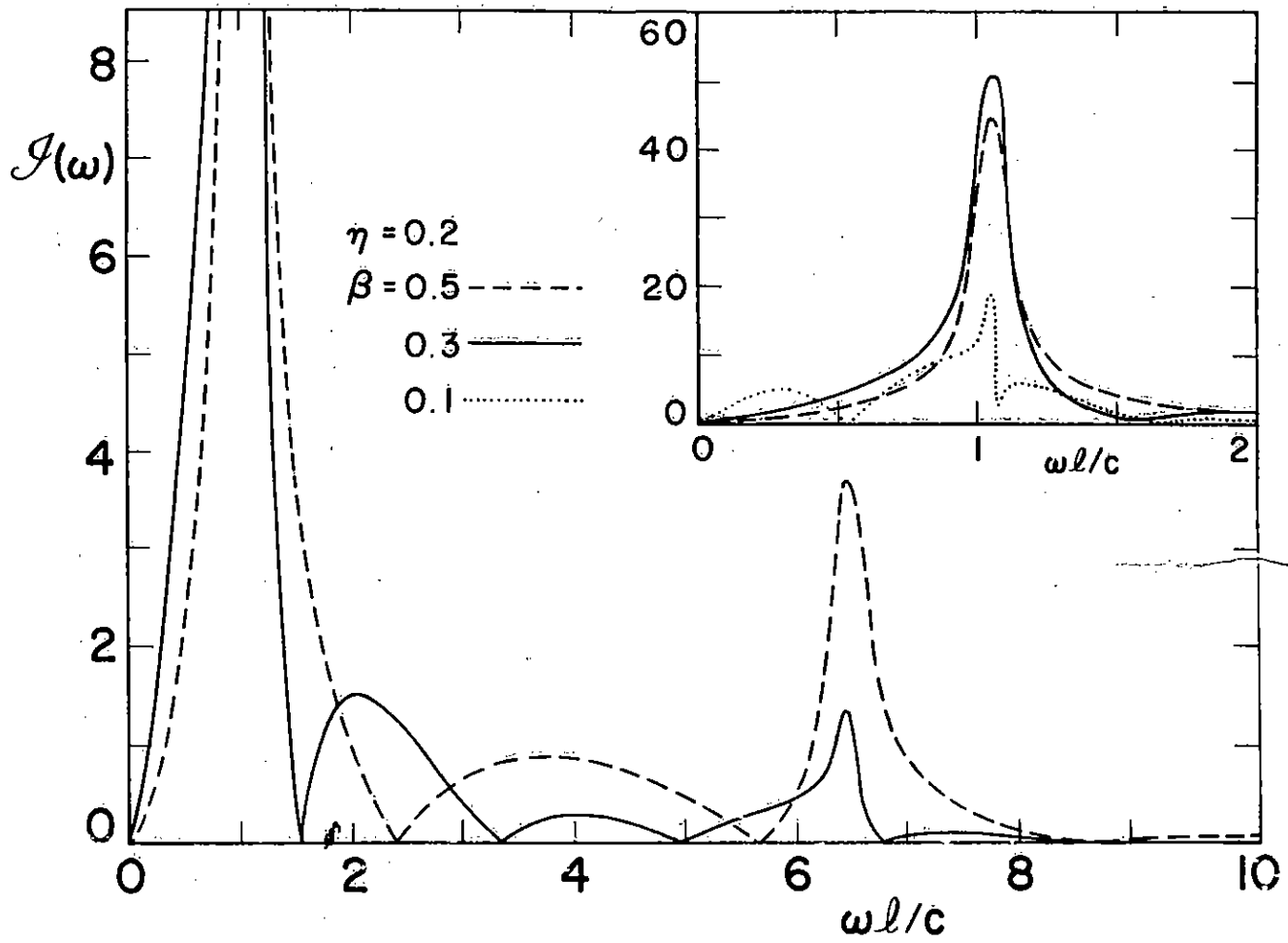

Figure 8b. Frequency Variation of Induced Current for $\eta = 0.2$

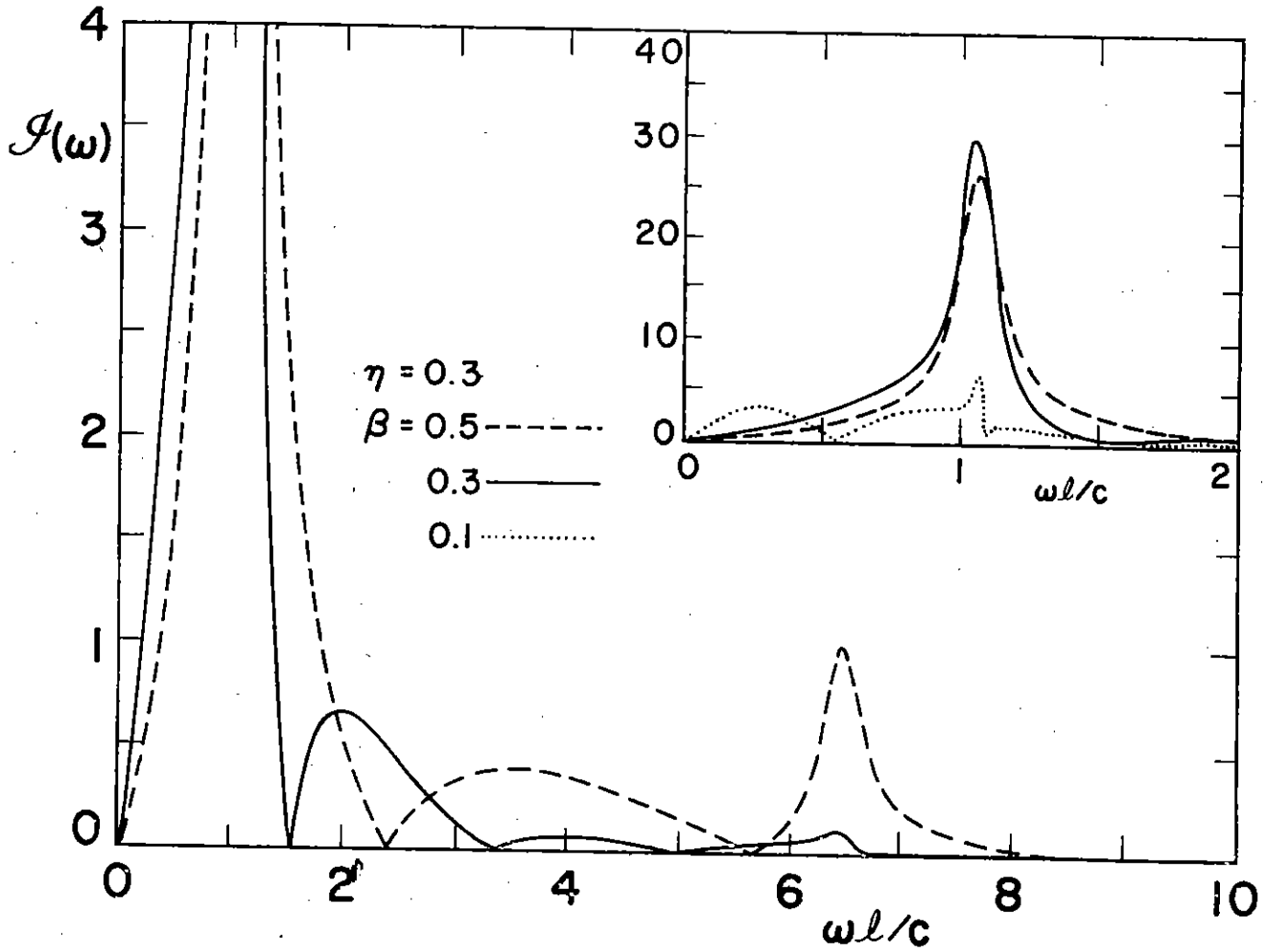

Figure 8c. Frequency Variation of Induced Current for $\eta = 0.3$

$$I(\ell/2,t) = -\frac{qv}{2\Omega\ell}\left[I_{\parallel}(\xi,\eta;\beta) + U(\xi)\sum_{n=1}^{\infty} I_n \cos(\nu_n^e\xi/\beta - \phi_n)\exp(-\delta_n^e\xi/\beta)\right.$$

$$\left. + U(\xi-1)\sum_{n=1}^{\infty} I_n \cos[\nu_n^e(\xi-1)/\beta + \phi_n]\exp[-\delta_n^e(\xi-1)/\beta] + O(\beta^2)\right] \tag{46}$$

where

$$I_n\exp(i\phi_n) = -\frac{8}{\beta^2} K_o[\eta\nu_n^e/(\gamma\beta)]$$

$$\frac{1 + i[d\nu_n^e/(\ell\beta\gamma^2) - \beta C_b/(C_s\nu_n^e)]}{\cos(\nu_n^e/2) + C_b\sin(\nu_n^e/2)/(C_s\nu_n^e) + 2\,C_b\cos(\nu_n^e/2)/[C_s(\nu_n^e)^2]} \tag{47}$$

$I_{\parallel}(\xi,\eta;\beta)$ is given by equation (20) and $U(t)$ is the Heaviside unit step function. The correction term $O(\beta^2)$ in equation (46) is negligible if the particle speed is not too large ($\beta < 0.5$) even when it is very close to the solar panels.

In figures 9a through 9c the time history of the normalized induced current $I(t)$,

$$I(t) = -\frac{2\Omega\ell}{qv} I(\ell/2,t)$$

is graphed at the midpoint of the boom with β and $\eta(=\rho_o/\ell)$ as parameters. Note that the time coordinate is expressed in terms of the normalized variable $\xi = vt/\ell$. From these curves one can see how the free oscillations of the satellite are excited by the moving particle and that the excitation is particularly strong when the particle is close to one of the solar panels. One also notes how these oscillations sustain themselves long after the particle has passed the satellite. Once the particle has passed both solar panels the current is a damped sinusoidal oscillation, showing that the fundamental resonance is sufficient to describe the induced current in the time region $t > \ell/v$. In these figures the fundamental resonance appears to be different for different values of β. This apparent difference is, of

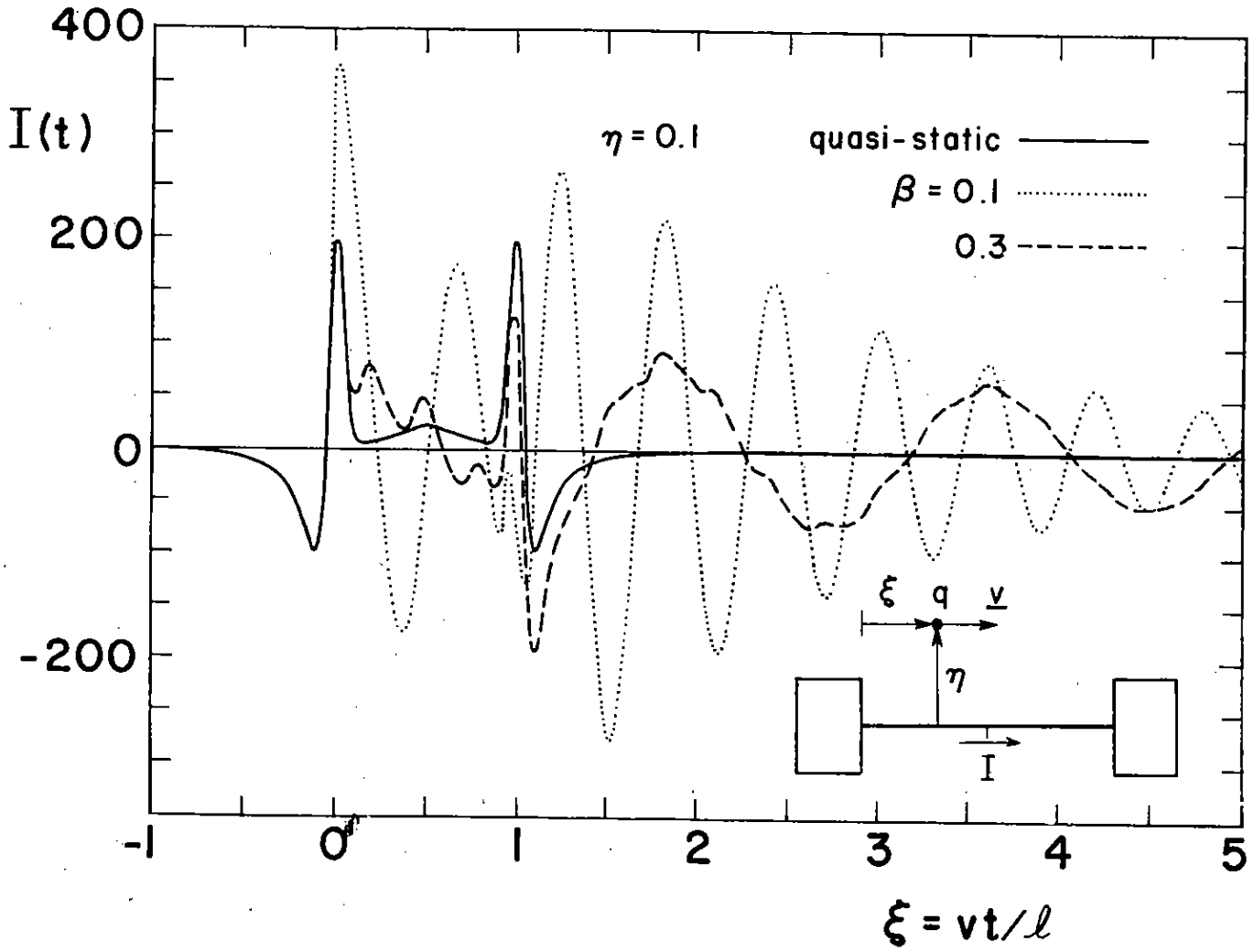

Figure 9a. Time History of Induced Current for $\eta = 0.1$

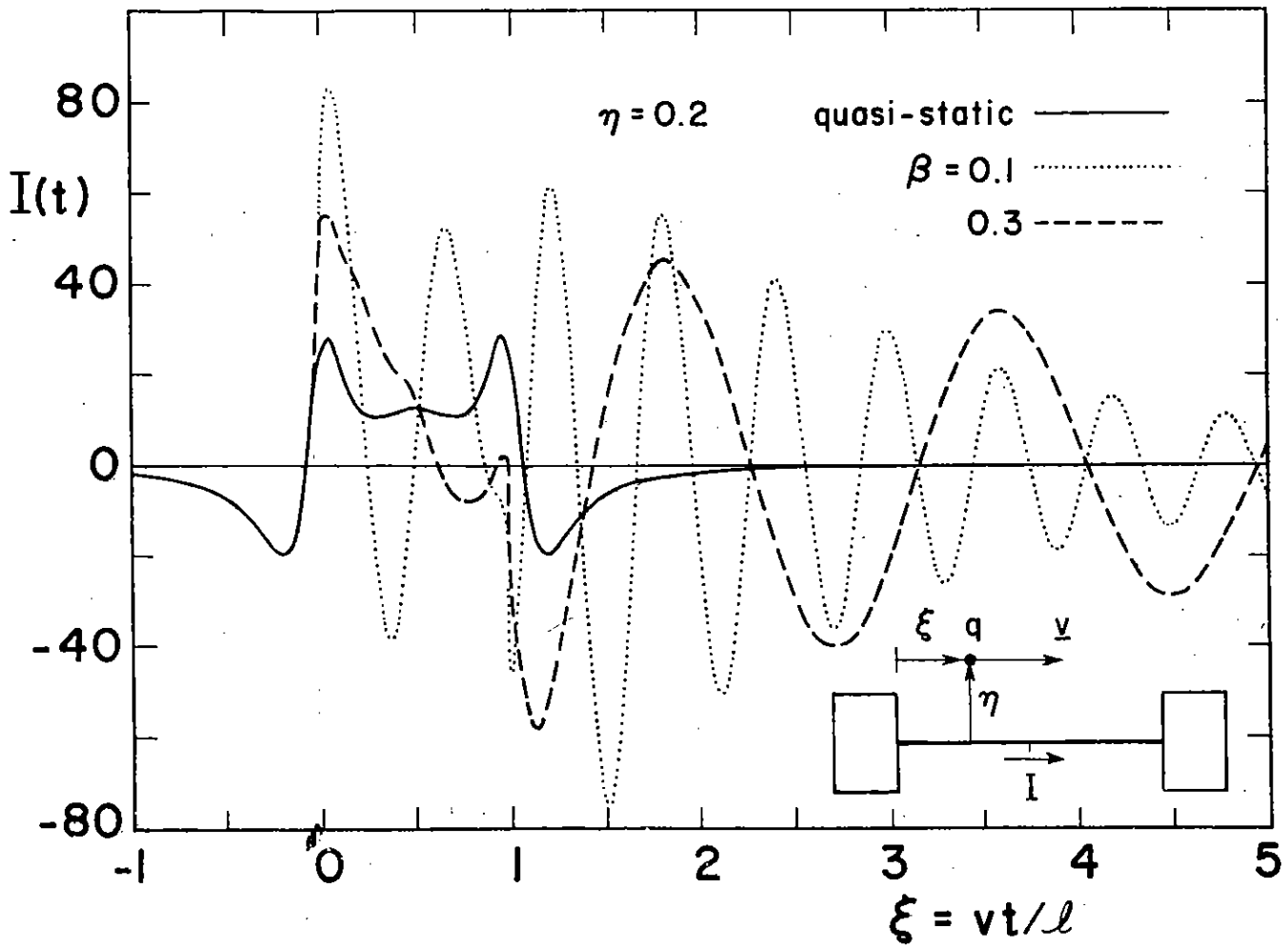

Figure 9b. Time History of Induced Current for $\eta = 0.2$

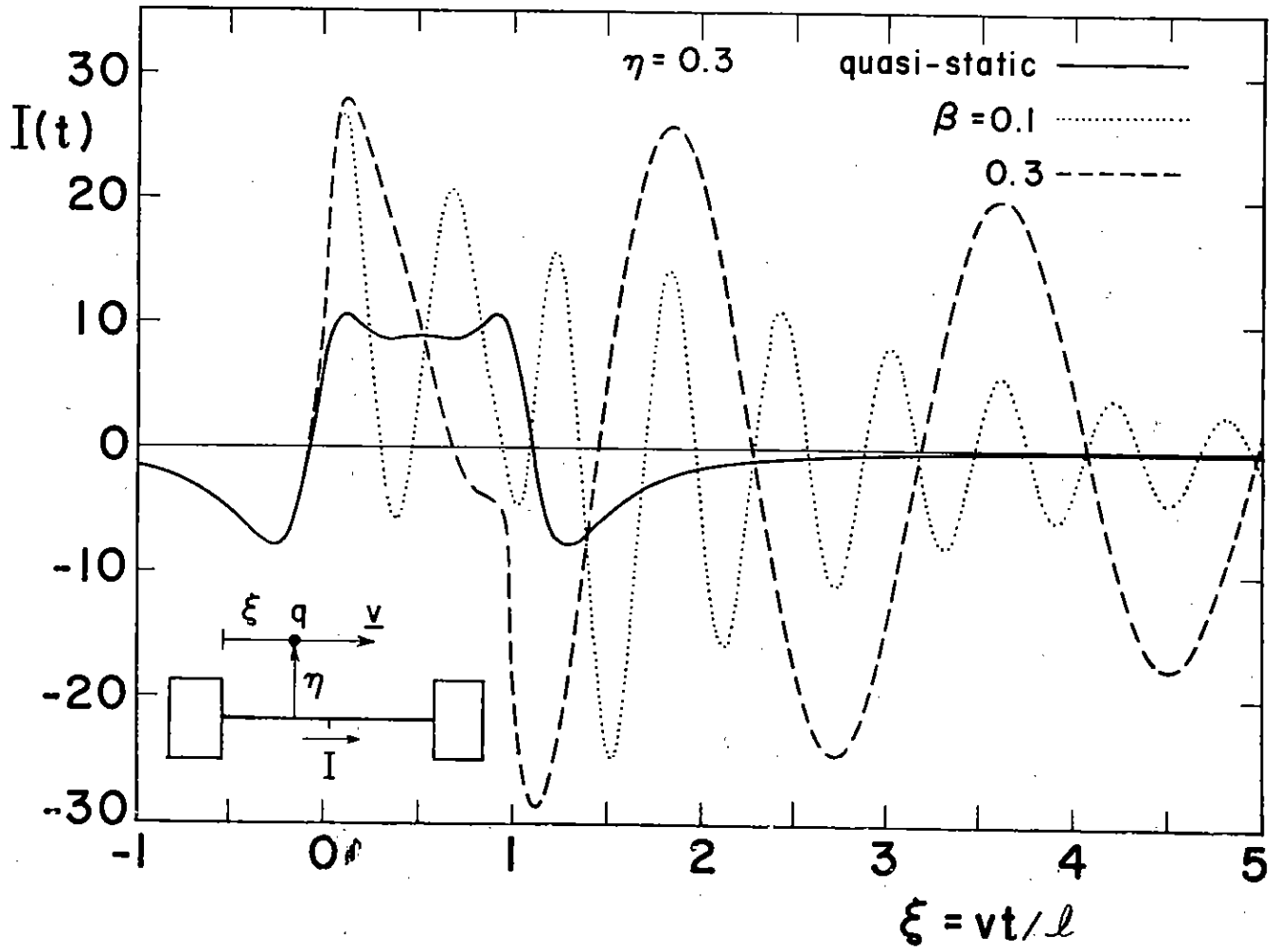

Figure 9c. Time History of Induced Current for $\eta = 0.3$

course, due to the fact that the time variable is expressed in terms of $\xi = vt/\ell$. When the current is plotted directly versus the time t these oscillations will have the same periodicity and damping constant.

Included in figures 9a through 9c are also the corresponding quasi-static results as given by equation (15). The graphs show that the difference between the quasi-static solution and the full-fledged dynamic solution is greater in this case than it is in the case of a thin wire. The important result of this section is that for system vulnerability assessments it is sufficiently adequate to include only the lowest resonance term in the sum (46) together with the quasi-static term. The latter term contributes mainly when the particle is close to the solar panels.

The behavior of the fundamental mode of the FLTSATCOM satellite studied in this report can be described by a RLC series network with some voltage generators. The inductance L and the capacitance C of this network have been calculated previously in this section, $L \simeq 11.8\ \mu H$ and $C = 55$ pF. The resistance is found from antenna theory to be $R = 49\ \Omega$. The voltage generators are, c.f. equation (28),

$$V(t) = \int_0^{\ell} E_z^{inc}(z,t)dz + d\,E_z^{inc}(0,t) + d\,E_z^{inc}(\ell,t) \qquad (48)$$

SECTION V

MANY-ELECTRON CALCULATION

So far only the effect of one moving charged particle has been treated in the calculations. These calculations can be used directly to treat the effect of a number of monoenergetic charged particles leaving the satellite at the same time and moving in the same direction. In the actual case where a photon pulse impinges upon the satellite the electrons are ejected at different directions and with different velocities. In this section, certain aspects of these actual features will be considered.

The following calculation is intended mainly to be an order-of-magnitude calculation and, hence, the quasi-static expression (15) for the induced currents will be used. A careful examination of equations (15) and (16) and figures 3 and 4 reveals that the induced current is described with sufficient accuracy by the expression

$$I(\tau) = - \frac{qv}{2\Omega\ell} \frac{C_s}{C_b} \left(\frac{1}{\tau^2} - \frac{2d \cos \psi}{\ell \tau^3} \right) U(\tau) \qquad (49)$$

where $\tau = (t-t')v/\ell$, ψ = angle between the boom and the particle's velocity $\underline{v}$, and $t = t'$ is the time when the charged particle leaves the solar panel at $z = 0$. It should be pointed out here that equation (49) is valid only for $v\tau > d/\ell$, where d has been defined on page 7. The reason is that the effects of the solar panels have been approximated by lumped network elements and generators throughout his report. Referring to figure 10 one can also express ψ in terms of θ and ϕ as follows:

$$\cos \psi = \sin \theta \cos \phi \qquad (50)$$

The energy distribution $f_e(E)$ (or, equivalently, the velocity distribution) of the emitted electrons is a function of the energy $h\nu$ of the incident photons and can be approximated with a triangular distribution:

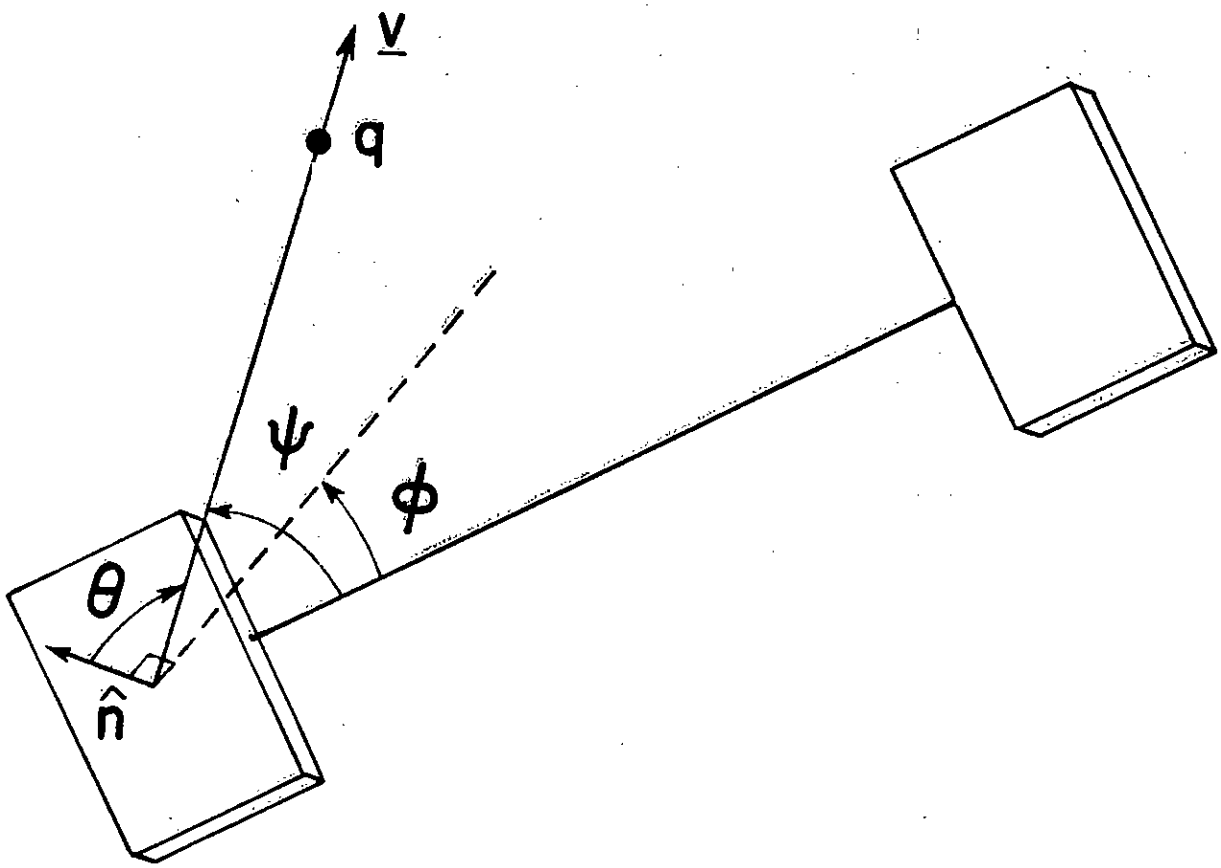

Figure 10. Angles Describing the Emitted Charge

$$f_e(E) = \begin{cases} 2E/(h\nu)^2, & E < h\nu \\ 0, & E > h\nu \end{cases} \tag{51}$$

where the electron kinetic energy $E \simeq mv^2/2$, m is the mass of the electron, ν is the frequency of the incident photon and h is Planck's constant. The yield f_y (i.e., the total number of electrons ejected by a photon with frequency ν) can be approximated as (references 8, 9)

$$f_y = (B/2)(h\nu)^{-\alpha} \tag{52}$$

where B and α are constants that depend on the material of the solar panels. Roughly, one has

$$\alpha \simeq 1.3, \qquad B \simeq 0.05 \tag{53}$$

and B is in unit of $(keV)^{\alpha}$. The number distribution f_ν of the incident photons can be described by that of a radiating black body, i.e.,

$$f_\nu(h\nu) = \frac{1}{2\zeta(3)} \frac{h^2\nu^2}{(kT)^3[\exp(h\nu/kT) - 1]} \tag{54}$$

where $\zeta(x)$ is the Riemann zeta function, T the absolute temperature and k Boltzmann's constant. Finally, the angular distribution f_Ω of the electrons is a cosine distribution from the normal of the panels, i.e.,

$$f_\Omega(\theta,\phi) = (2\pi)^{-1}\cos\theta \tag{55}$$

Let the total number of photons in the pulse be N_ν and the shape of the pulse $f(t)$ be triangular so that

$$f(t) = \begin{cases} 0, & t < 0 \\ t/t_o^2, & 0 < t < t_o \\ (2t_o - t)/t_o^2, & t_o < t < 2t_o \\ 0, & t > 2t_o \end{cases} \tag{56}$$

A typical value of t_o is 10 ns, i.e., the pulse width is 20 ns. Combining equations (49)-(56) one has

$$I(t) = \int \frac{N_\nu q \ell \sqrt{m}}{2\Omega\sqrt{2E}} \frac{C_s}{C_b} \frac{1}{(t-t')^2} \left[1 - \frac{2d\sqrt{m}\cos\theta\cos\phi}{\sqrt{2E}\,(t-t')}\right]$$

$$f_\Omega(\theta,\phi) f_e(E) f_y(h\nu) f_\nu(h\nu) f(t') \sin\theta\, d\theta d\phi dE\, d(h\nu) dt' \qquad (57)$$

Since only back-scattered electrons are of importance here, the angular domain of integration in equation (57) is $0 \le \theta \le \pi/2$, $0 \le \phi \le 2\pi$. Performing the integrals in the following order: (1) the θ,ϕ-integration, (2) the E-integration, (3) the $h\nu$-integration, and (4) and t'-integration one obtains

$$I(t) = \frac{N_\nu q \ell}{2\Omega c} \sqrt{\frac{mc^2}{2}} \frac{C_s}{C_b} \int \frac{1}{(t-t')^2} \frac{1}{\sqrt{E}} f_e(E) f_y(h\nu) f_\nu(h\nu) f(t') dE\, d(h\nu) dt'$$

$$= \frac{2N_\nu q \ell}{3\Omega c} \sqrt{\frac{mc^2}{2}} \frac{C_s}{C_b} \int \frac{1}{(t-t')^2} \frac{1}{\sqrt{h\nu}} f_y(h\nu) f_\nu(h\nu) f(t') d(h\nu) dt'$$

$$= \frac{N_\nu q \ell}{6\Omega c} \frac{\zeta(5/2-\alpha)\Gamma(5/2-\alpha)}{\zeta(3)} \frac{C_s}{C_b} \sqrt{\frac{mc^2}{2kT}} \frac{B}{(kT)^\alpha} \int_0^{2t_o} \frac{1}{(t-t')^2} f(t') dt'$$

$$= \frac{N_\nu q \ell}{6\Omega c t_o^2} \frac{\zeta(5/2-\alpha)\Gamma(5/2-\alpha)}{\zeta(3)} \frac{C_s}{C_b} \sqrt{\frac{mc^2}{2kT}} \frac{B}{(kT)^\alpha} \ell n \left[\frac{(t-t_o)^2}{t(t-2t_o)}\right], \quad t > 2t_o \qquad (58)$$

Note that the result (58) is valid only for $t > 2t_o$ since the t'-integration converges only for $t > 2t_o$. Again, this is due to the lumped network model for the solar panels. Using appropriate values for the constants in equation (58) one gets

$$I(t) = 2.67\times10^{-12} N_\nu (kT)^{-1.8} \ell n \left[\frac{(1-10/t)^2}{1-20/t}\right], \quad t > 20 \text{ ns} \qquad (59)$$

where I is in amperes, kT in keV, t in ns. For kT = 1 keV one has

$$I(t) = 2.7\times10^{-12}\ N_\nu\ \ell n\left[\frac{(1-10/t)^2}{1-20/t}\right], \qquad t > 20\ \text{ns} \tag{60}$$

With a photon flux of $10^{16}/m^2$ per pulse and kT = 1 keV one gets (c.f. reference 10)

$$\begin{aligned} I(t) &= 1.6\times10^{5}\ \ell n\left[\frac{(1-10/t)^2}{1-20/t}\right], \qquad t > 20\ \text{ns} \\ &\simeq 1.6\times10^{6}\ t^{-2}, \qquad\qquad t > 50\ \text{ns} \end{aligned} \tag{61}$$

The time dependence of the current pulse is shown in figure 11. In this figure the current pulse is plotted for $t \geq 30$ ns, since on physical grounds equation (61) is expected to be valid for $t > 30$ ns. The parameters of the incident photon pulse chosen for this numerical sample calculation corresponds to a flux level of 10^{-4} cal/cm^2. From the above low-fluence calculations one notes that the amplitude of the induced current pulse on the boom can be of the order of hundreds of kiloamperes and that the width of the current pulse is considerably larger than the width of the incident photon pulse.

The above calculations are based on a quasi-static expression for the induced current. Since the chosen photon pulse width is of the order of the transit time along the satellite under consideration, the calculations might not be reliable. However, judging from figures 9a - 9c one can say that the quasi-static solution still yields the correct order-of-magnitude calculation for the induced currents. For a more accurate pulse shape and frequency variation of the induced boom currents, the calculations performed in this section have to be extended to include the effects of the lowest resonance of the satellite. Unfortunately, such an extension is considerably more complicated and is beyond the scope of the present investigation. Because of its importance, however, it should be carried out in a future investigation.

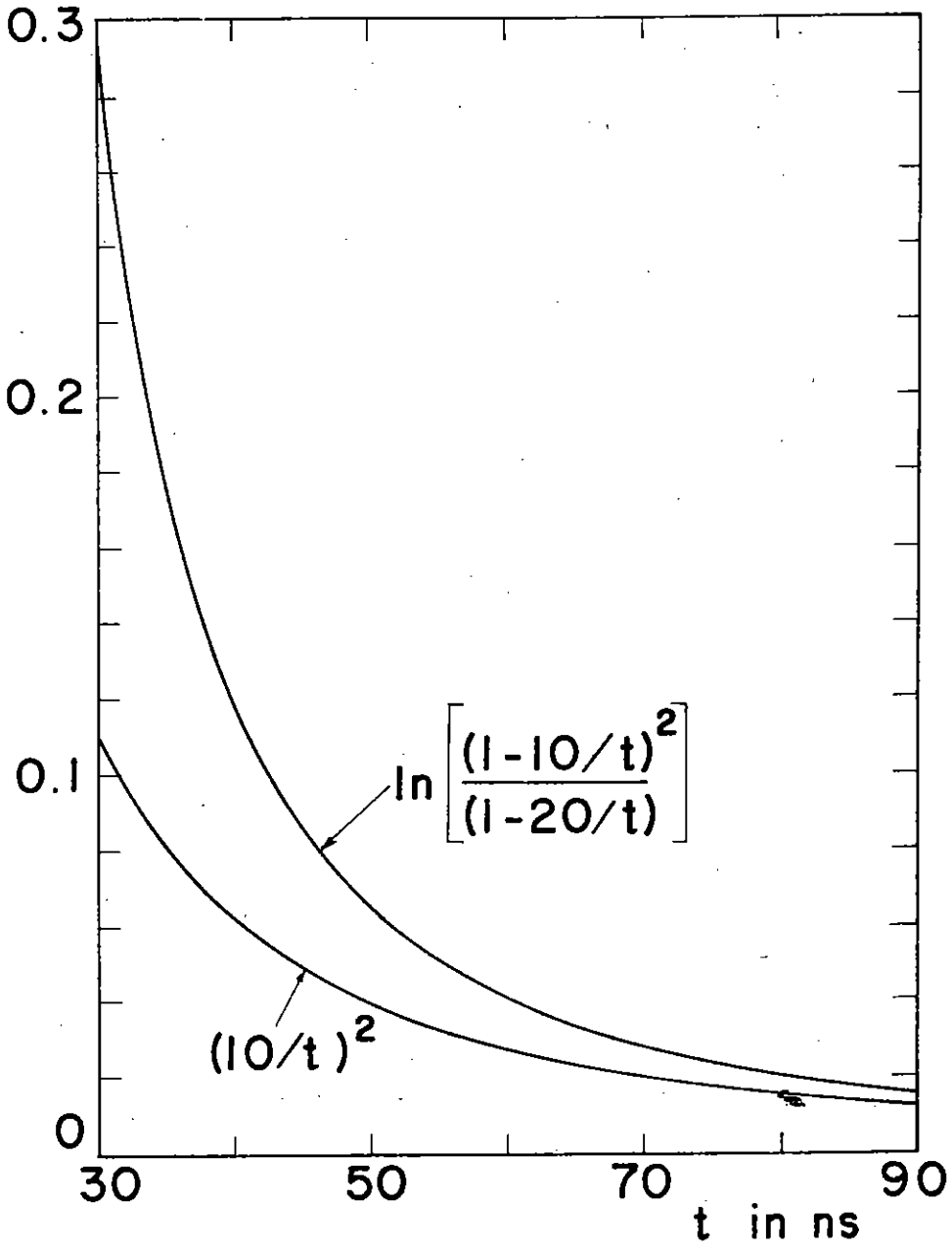

Figure 11. Current-Pulse Shape from Low-Fluence Calculation

SECTION VI

CURRENTS RESULTING FROM REDISTRIBUTION OF NET CHARGES ON SOLAR PANELS

When a photon pulse strikes the satellite, as depicted in figure 2, a majority of the emitted electrons come from the solar panels because of their relatively large surfaces and, hence, each panel is left with some positive net charge. This charge redistributes itself over the entire satellite and in so doing currents are induced. To get an estimate of these currents it will be assumed that one solar panel is bombarded by a short photon pulse (at $t = 0$) and that the net charge on the panel immediately after the passage of the photon pulse is Q. The following calculations will show the importance of including the effects of net charges on the satellite in any type of self-consistent calculations.

The problem under consideration can be formulated mathematically as follows. The initial net charge on the solar panel at $z = 0$ is Q. In accordance with the discussions in section II this initial condition means that

$$E_z^{inc}(t=0+) = \frac{Q}{C_s}\,\delta(z) \tag{62}$$

The situation is similar to that of discharging a capacitance into a transmission line. The boom current then satisfies the integro-differential equation

$$\left(\frac{d^2}{dz^2} - \frac{s^2}{c^2}\right)\int_0^{\ell} \frac{\exp(-sR/c)}{4\pi R}\, I(z',s)\,dz' = \frac{\varepsilon}{C_s}\left\{[I(0,s) - Q]\delta(z) + I(\ell,s)\delta(z-\ell)\right\} \tag{63}$$

together with the end conditions

$$\frac{dI}{dz} = 0, \qquad z = 0,\ell \tag{64}$$

Or, equivalently,

$$\int_0^{\ell} \frac{\exp(-sR/c)}{4\pi R} I(z',s)dz' = A \cosh \frac{sz}{c} + B \sinh \frac{sz}{c} \tag{65}$$

together with the end conditions

$$\begin{aligned} \frac{d}{dz} I(0,s) &= \frac{C_b}{\ell C_s} [I(0,s) - Q] \\ \frac{d}{dz} I(\ell,s) &= - \frac{C_b}{\ell C_s} I(\ell,s) \end{aligned} \tag{66}$$

The solution of equations (63) and (64), or equations (65) and (66), is

$$I(z,s) = - \frac{\varepsilon Q}{C_s} \sum_n \frac{1}{s-s_n} \frac{I_n(0)}{B_n} I_n(z) \tag{67}$$

and at $z = \ell/2$ one has

$$I(\ell/2,s) = \frac{Qc}{\ell} \frac{C_b}{C_s} \sum_n \frac{\cosh(s_n^e \ell/2c)}{s-s_n^e} \frac{1}{(s_n^e \ell/c) + \sinh(s_n^e \ell/c)} \tag{68}$$

The frequency variation of the current at the midpoint of the boom is then

$$I(\ell/2,\omega) = Q \frac{C_b}{C_s} \sum_{n=1}^{\infty} \left[\frac{1}{(\omega\ell/c)+\nu_n^e+i\delta_n^e} - \frac{1}{(\omega\ell/c)-\nu_n^e+i\delta_n^e} \right] \frac{\cos(\nu_n^e/2)}{\nu_n^e + \sin \nu_n^e} \tag{69}$$

When ω is not close to a resonance frequency, the induced current $I(\ell/2,\omega)$ is expressible in the following closed form:

$$I(\ell/2,\omega) = \frac{Q}{2}\frac{C_b}{C_s}\frac{1}{(C_b/C_s)\cos(\omega\ell/2c) - (\omega\ell/c)\sin(\omega\ell/2c)} \tag{70}$$

When ω is close to the resonance frequency ω_n^e the sum can be approximated by one term, namely,

$$I(\ell/2,\omega) \simeq - Q\frac{C_b}{C_s}\frac{1}{(\omega\ell/c) - \nu_n^e + i\delta_n^e}\frac{\cos(\nu_n^e/2)}{\nu_n^e + \sin\nu_n^e}$$

The normalized quantity

$$I_Q(\omega) = \frac{\Omega}{2Q} I(\ell/2,\omega) \tag{72}$$

is graphed in figure 12. A comparison between figures 8a - 8c and figure 12 reveals that the currents induced by the moving electrons are of the same order of magnitude as those induced by the "holes" left behind by the emitted electrons.

The inverse Laplace transform of equation (68) gives the following time-domain representation of the induced boom current:

$$I(\ell/2,t) = -\frac{2Qc}{\ell}\frac{C_b}{C_s}\sum_{n=1}^{\infty}\frac{\cos(\nu_n^e/2)\sin(\omega_n^e t)\exp(-\alpha_n^e t)}{\nu_n^e + \sin\nu_n^e}$$

$$= \frac{2Qc}{\ell}\frac{C_b}{C_s}\sum_{n=1}^{\infty}\frac{\sin(\omega_n^e t)\exp(-\alpha_n^e t)}{[(C_b/C_s) + 2]\sin(\nu_n^e/2) + \nu_n^e\cos(\nu_n^e/2)} \tag{73}$$

In figures 13a - 13b the normalized quantity

$$i_Q(t) = \frac{2\ell\Omega}{Qc} I(\ell/2,t) \tag{74}$$

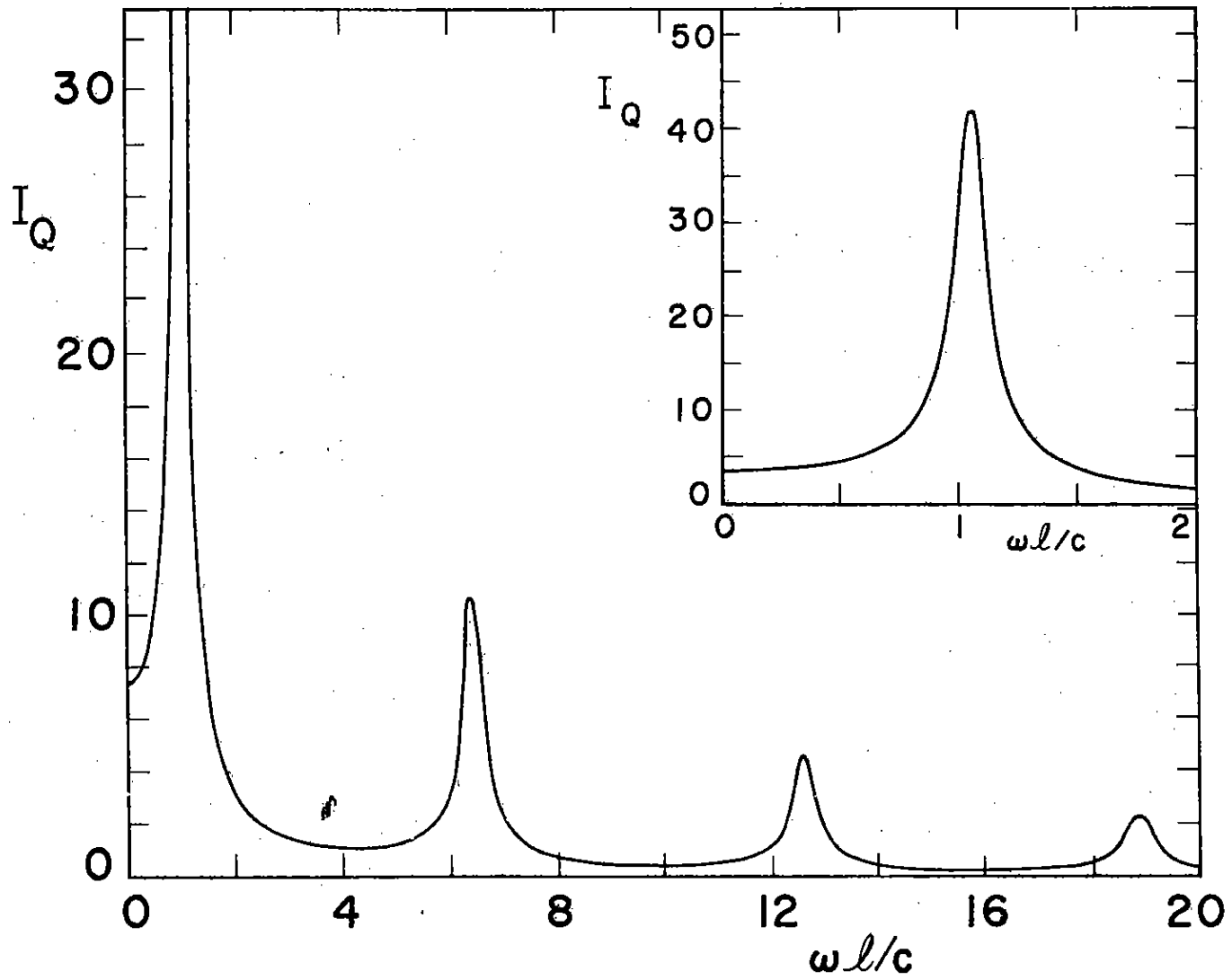

Figure 12. Frequency Variation of Normalized Current from Redistribution of Net Charges on Solar Panels

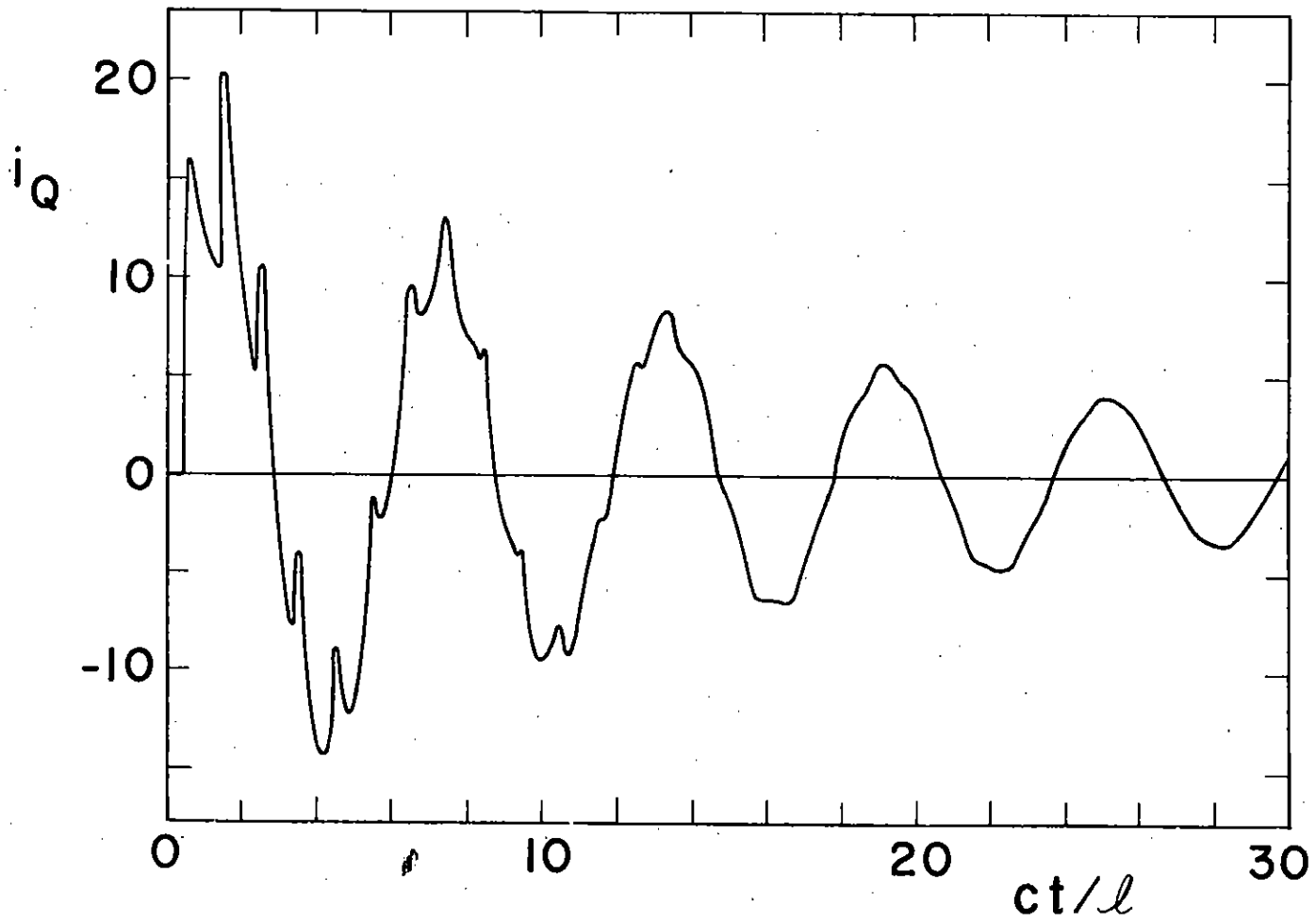

Figure 13a. Time History of Normalized Current from Redistribution of Net Charges on Solar Panels

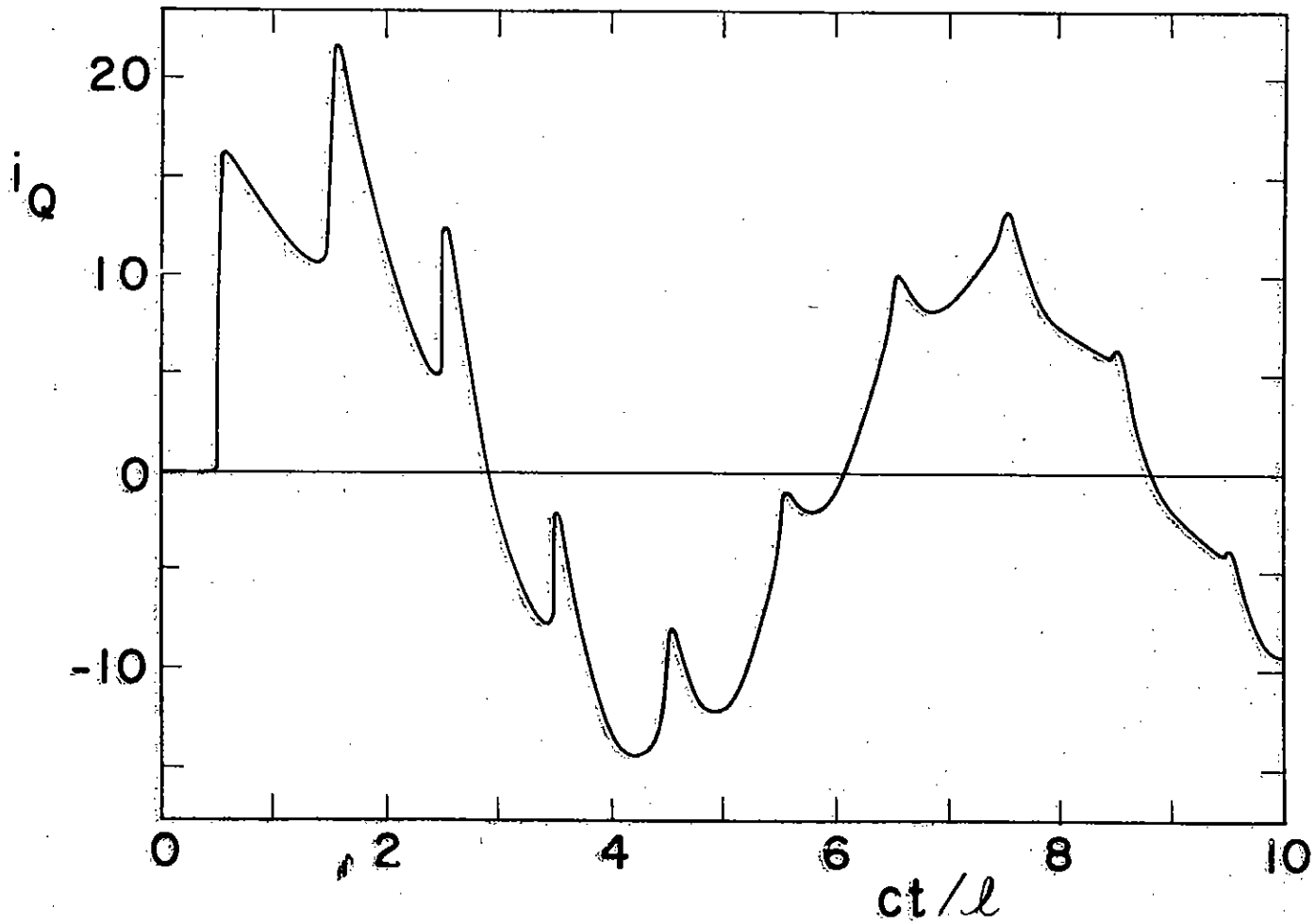

Figure 13b. Early Time Behavior of Normalized Current from Redistribution of Net Charges on Solar Panels

is plotted versus time. It is observed from these figures that the first resonance alone accounts for much of the induced current after only 3 transit times of the satellite.

SECTION VII

SOME RELATED CONSIDERATIONS

In this section a brief discussion is given of some special aspects concerning the influence of the central cylinder.

The lowest even resonances that have been calculated in section IV are not affected appreciably by the presence of the central cylinder when the cylinder is in electrical contact with the boom. The reason is that the charge density vanishes at the midpoint of the boom for the even resonances. On the other hand, the charge density of the odd modes has a local maximum at the center of the boom. It is therefore expected that mainly the odd resonances in section IV are affected by the central cylinder.

When the boom and the central cylinder are in direct electrical contact with each other, the method used in sections II and IV to calculate the current on the entire boom can be applied to each section of the boom that connects the solar panels with the central cylinder. After some algebraic manipulations one obtains the following transcendental equation from which the odd resonances can be calculated:

$$s_n^o: \quad \frac{s\ell}{c} \coth \frac{s\ell}{2c} + \left[\left(\frac{s\ell}{c}\right)^2 + \frac{2C_b^2}{C_s C_c}\right]\left[\frac{C_b}{C_s} + \frac{2C_b}{C_c}\right]^{-1} = 0 \tag{75}$$

where C_c is the capacitance of the central cylinder. With the height and and diameter of the central cylinder both being 2m one has $C_c/C_b \simeq 2.20$ and, as before, $C_s/C_b \simeq 1.62$. For large values of $|s|$ one can expand s_n^o in the asymptotic series

$$s_{n+1}^o \simeq \pm \frac{ic}{\ell}\left(2n\pi + \frac{3.06}{2n\pi} - \frac{10.04}{(2n\pi)^3}\right) \tag{76}$$

The ten lowest resonances as given by a numerical solution of equation (75) are

$$s_n^o = \pm i(c/\ell)\nu_n^o \tag{77}$$

n	1	2	3	4	5	6	7	8	9	10
ν_n^o	1.69	6.73	12.80	19.01	25.25	31.51	37.78	44.05	50.33	56.60

The asymptotic form (76) agrees within 0.5% with the numerical solution of equation (75) except for $n = 1$.

The lowest resonance frequency can be obtained from a network description of the satellite as shown in figure 14. The resonance frequency ω_r of this network is given by

$$\omega_r = \left[\frac{1}{L_b}\left(\frac{1}{C_s} + \frac{2}{C_c}\right)\right]^{1/2} \simeq 1.8\,\frac{c}{\ell} \tag{78}$$

which agrees within 6% with the lowest odd resonance frequency of the satellite given in the table.

It can be seen from the table here and that given in section IV that the odd resonance frequencies are lowered by the central cylinder. This effect can be understood from the fact that the current of the odd modes vanishes at the midpoint of the boom when the central cylinder is absent, whereas in the presence of the central cylinder this is not the case. In the latter case one can allow some net current to flow into the cylinder from the boom on either side of the cylinder. This net current gives rise to some net charge on the cylinder. To calculate the effects of these charges is beyond the scope of the present report and has to be left to a future investigation.

The entire satellite as seen from the terminals between the two points where the boom intersects the central cylinder can be considered as a receiving antenna center-loaded with the cylinder. Two quantities that uniquely describe the antenna at the terminals are the input admittance and the short-circuit current. The short-circuit current is the current induced

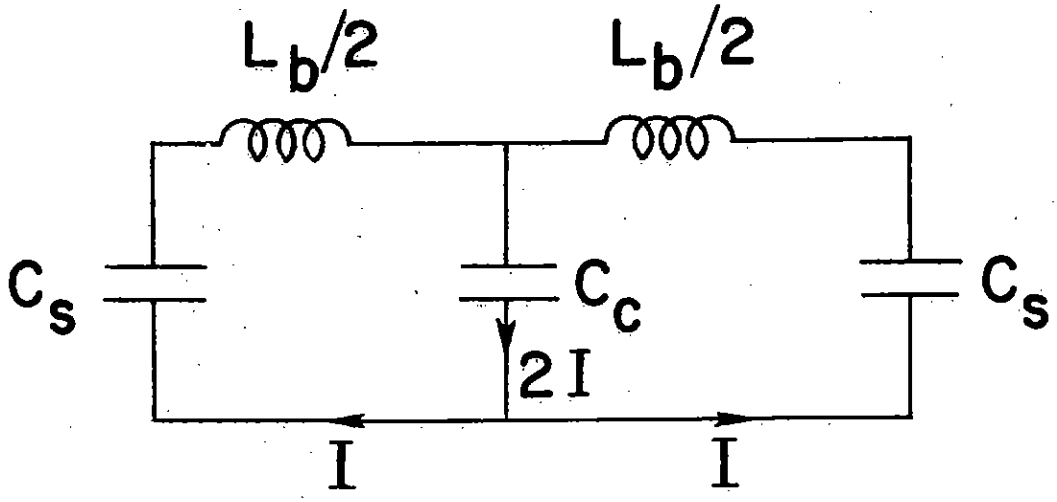

Figure 14. Network Representation of the Lowest Odd Resonance of a FLTSATCOM Satellite

by the moving electrons when the central cylinder is absent and the two halves of the boom are connected. This current has been calculated in section IV.

The input admittance of the antenna can be calculated with the aid of the thin-wire model of the boom together with the end conditions derived in section II. Some algebraic manipulations similar to those in section IV give the following expression for the input admittance:

$$Y_{in}(\omega) = \frac{4\pi}{i\Omega Z_o} \sum_{n=1}^{\infty} \frac{\omega \omega_n^e}{(\omega + i\alpha_n^e)^2 - (\omega_n^e)^2} \frac{1}{\nu_n^e - \sin \nu_n^e} \tag{79}$$

When ω is near ω_n^e, the most important term in the sum is

$$Y_{in}(\omega) \simeq \frac{2\pi}{i\Omega Z_o} \frac{\omega_n^e}{\omega - \omega_n^e + i\alpha_n^e} \frac{1}{\nu_n^e - \sin \nu_n^e} \tag{80}$$

If $|\omega - \omega_n^e| >> \alpha_n^e$ then the influence of α_n^e can be neglected and the simplified sum thus obtained for Y_{in} can be summed in a closed form as follows:

$$Y_{in}(\omega) = \frac{2\pi i}{\Omega Z_o} \frac{\sin(\omega \ell/2c) + (\omega \ell C_s/cC_b)\cos(\omega \ell/2c)}{\cos(\omega \ell/2c) - (\omega \ell C_s/cC_b)\sin(\omega \ell/2c)} \tag{81}$$

The frequency variation of the input admittance is graphed in figure 15. The normalized quantity presented in this figure is $Z_b Y_{in}$, where Z_b is the characteristic impedance of the boom, $Z_b = Z_o \Omega/4\pi$.

The current I flowing through the central cylinder is given by

$$I = I_{sc}/(1 + Z_c Y_{in}) \tag{82}$$

where I_{sc} is the short-circuit current calculated in section IV and Z_c is the impedance presented by the central cylinder at the terminals.

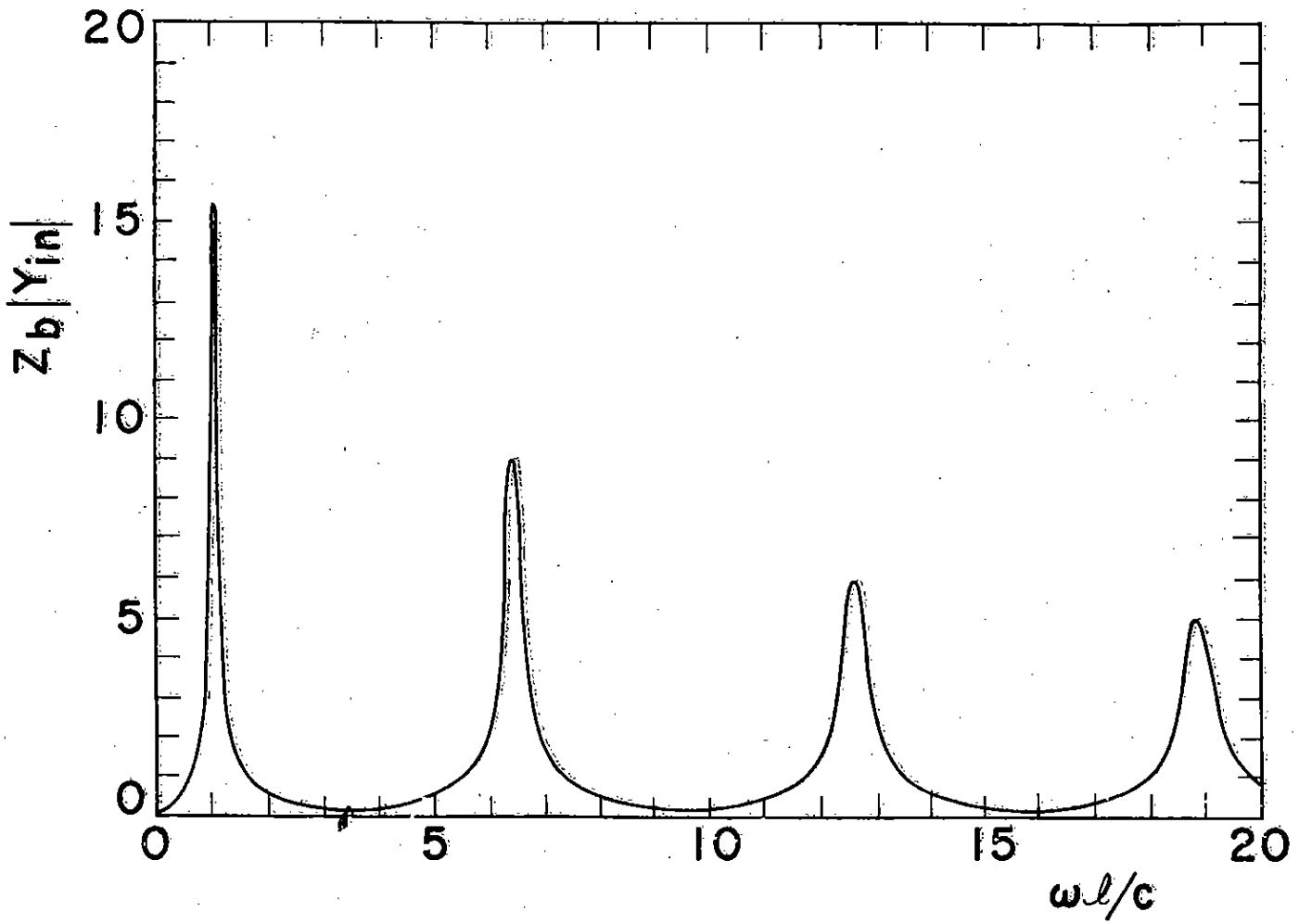

Figure 15. Frequency Variation of Normalized Input Admittance of the Solar Panels and the Boom Seem from the Central Cylinder

SECTION VIII

SUMMARY, CONCLUSIONS, AND SUGGESTIONS

The method of solution employed in this report is summarized in figure 16. A rigorous integral equation for the induced surface currents on the entire satellite is first written down with the incident tangential electric field as the source term of the equation. This source term can be either the field of the ejected electrons moving outside the satellite or the net charge left behind by the electrons on the satellite. To make the integral equation analytically tractable a simplified integral equation for the boom current is obtained in which the effects of the solar panels and the central cylinder are duplicated by some localized generators driving, and some lumped impedances loading the boom. This simplified integral equation is subsequently solved analytically after splitting the boom current into its even and odd parts with respect to the central cylinder. The quasi-static and dynamic solutions for one moving charged particle are obtained and compared. The boom current arising from the redistribution of the net positive charge on the satellite is calculated from the simplified integral equation. The quasi-static solution for one particle is then utilized to obtain, by superposition, the solution of the many-electron problem for a given incident photon pulse, a given yield function, and a given angular and energy distribution of the ejected electrons.

The important findings of this investigation are as follows:

1. The quasi-static solution is in general not sufficiently accurate. When the electron is less than one meter away from either solar panel, the peak value of the boom current is within a factor of two from the peak value of the dynamic solution for electron's energy less than 20 keV. For higher electron energies and greater distances away from the satellite the quasi-static solution can be off by orders of magnitude.
2. For $\beta > 0.15$ (electron's energy > 5.6 keV) the fundamental mode alone accounts for at least 90% of the energy contained in all the even current modes, whereas for $\beta < 0.15$ the fundamental mode together with

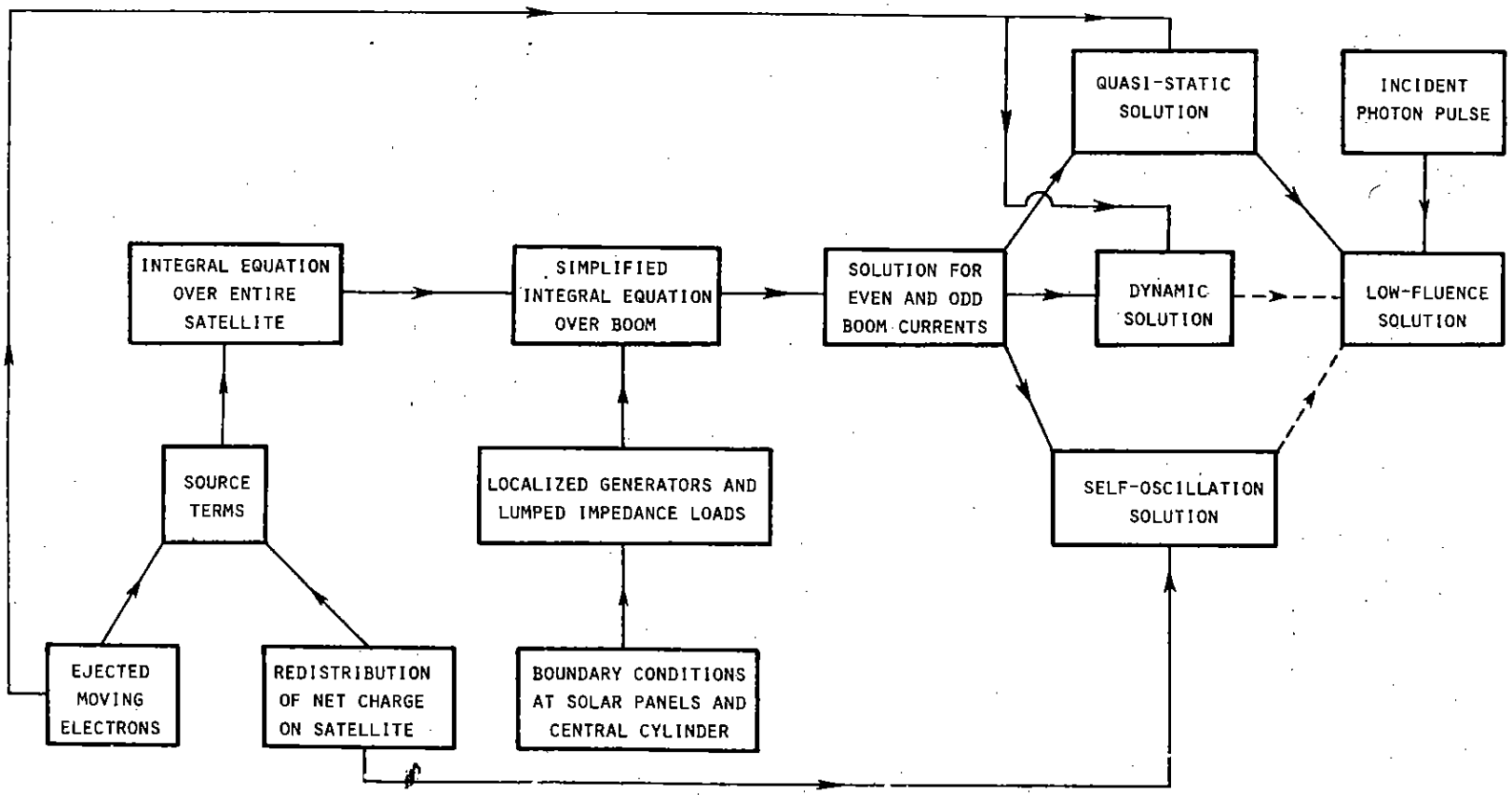

Figure 16. Block Diagram Depicting the Method of Solution Employed in this Report

quasi-static solution accounts for the same percentage of energy.

3. The wavelengths of the even and odd fundamental modes are, respectively, about three and four times those of the corresponding modes of a thin wire whose length equals that of the boom. This increase in the resonance wavelengths implies that the induced current continues to oscillate with significant amplitude even long after the photon pulse has passed the satellite.
4. The even fundamental mode can be excited to a comparable extent by the moving electrons and by the redistribution of the positive net charge on the satellite left behind by the ejected electrons.
5. The fundamental mode of the boom current can be calculated with sufficient accuracy from a RLC network excited by two types of voltage generators, one type accounting directly for the field of the moving electrons and the other for the induced currents and charges on the solar panels and the central cylinder. The resistance R has to be computed from antenna theory, while L and C are respectively the inductance of the boom and the capacitance between the solar panels and the central cylinder.
6. The time history of the boom current is calculated, by superposition, in terms of the total number N_ν and temperature T of an incident photon pulse. For $N_\nu = 10^{16}$ photons per square meter and $kT = 1$ keV (these data correspond to a flux level of 10^{-4} cal/cm^2), the peak current is of the order of hundreds of kiloamperes.

It appears that since the fundamental mode alone is very close to the true dynamic solution, the most natural and important extension of the present work is to make use of the results on the fundamental mode to calculate the low-fluence response of the satellite. Such a calculation will consist of two parts: one part is associated with the redistribution of the positive net charge on the satellite and the other part deals with the effect of electrons moving outside the satellite. This suggested direction for extension is indicated in figure 16 by broken lines. Another important direction for immediate investigation is to seek a set of self-consistent equations for the determination of the amplitude of the fundamental mode. The end result of this report

will be the natural point of departure for such an investigation, since all the properties of the fundamental mode have been found.